2018-12

SUBMUNITION DESIGN FOR A LOW-COST SMALL UAS COUNTER-SWARM MISSILE

Lobo, Keith

Monterey, CA; Naval Postgraduate School

NAVAL POSTGRADUATE SCHOOL

MONTEREY, CALIFORNIA

THESIS

SUBMUNITION DESIGN FOR A LOW-COST SMALL UAS COUNTER-SWARM MISSILE

by

Keith B. Lobo

December 2018

Thesis Advisor:	Christopher M. Brophy
Co-Advisor:	Robert G. Wright
Second Reader:	Christopher A. Adams

THIS PAGE INTENTIONALLY LEFT BLANK

REPORT DOCUMENTATION PAGE			*Form Approved OMB No. 0704-0188*

1. AGENCY USE ONLY *(Leave blank)*	**2. REPORT DATE** December 2018	**3. REPORT TYPE AND DATES COVERED** Master's thesis

4. TITLE AND SUBTITLE SUBMUNITION DESIGN FOR A LOW-COST SMALL UAS COUNTER-SWARM MISSILE	**5. FUNDING NUMBERS**
6. AUTHOR(S) Keith B. Lobo	
7. PERFORMING ORGANIZATION NAME(S) AND ADDRESS(ES) Naval Postgraduate School Monterey, CA 93943-5000	**8. PERFORMING ORGANIZATION REPORT NUMBER**
9. SPONSORING / MONITORING AGENCY NAME(S) AND ADDRESS(ES) N/A	**10. SPONSORING / MONITORING AGENCY REPORT NUMBER**

11. SUPPLEMENTARY NOTES The views expressed in this thesis are those of the author and do not reflect the official policy or position of the Department of Defense or the U.S. Government.

12a. DISTRIBUTION / AVAILABILITY STATEMENT Approved for public release. Distribution is unlimited.	**12b. DISTRIBUTION CODE** A

13. ABSTRACT (maximum 200 words)

The emergence of high-performance, consumer-grade, and low-cost drones (under $1000), combined with artificial intelligence and low-cost computer processing power, has provided the tools and platforms on which to build drone swarms. In the context of recent weaponization of commercially available unmanned aerial systems (UAS) such as quadcopters, these trends present two major challenges: the possibility of defenses getting overwhelmed and the large cost asymmetry between currently available defenses and the cost of these threats.

Survivability methodology was used to study the susceptibility and vulnerability of threat vehicles. This analysis was then used to design and develop a submunition possessing a low-cost kill mechanism, such that multiple units could be delivered by a low-cost delivery vehicle. Vulnerability analysis revealed that a fouling mechanism would be highly effective and was therefore chosen as the kill mechanism. The submunition's aerodynamics were modeled and used to develop a concept of operations involving the deployment of multiple submunitions from a single delivery vehicle. The kill mechanism, submunition, and delivery vehicle were manufactured using commercially available components and additive manufacturing. Experimental testing has demonstrated the viability of these designs and the ability to provide a defense against small UAS swarms with low-cost technologies.

14. SUBJECT TERMS counter-swarm, UAV, UAS, low-cost, weapon, payload, submunition, design	**15. NUMBER OF PAGES** 81
	16. PRICE CODE

17. SECURITY CLASSIFICATION OF REPORT	**18. SECURITY CLASSIFICATION OF THIS PAGE**	**19. SECURITY CLASSIFICATION OF ABSTRACT**	**20. LIMITATION OF ABSTRACT**
Unclassified	Unclassified	Unclassified	UU

NSN 7540-01-280-5500

Standard Form 298 (Rev. 2-89)
Prescribed by ANSI Std. 239-18

THIS PAGE INTENTIONALLY LEFT BLANK

Approved for public release. Distribution is unlimited.

SUBMUNITION DESIGN FOR A LOW-COST SMALL UAS COUNTER-SWARM MISSILE

Keith B. Lobo
Captain, Royal Canadian Air Force
BEng, Ryerson University, 2003

Submitted in partial fulfillment of the
requirements for the degrees of

MASTER OF SCIENCE IN MECHANICAL ENGINEERING

and

MASTER OF SCIENCE IN ASTRONAUTICAL ENGINEERING

from the

NAVAL POSTGRADUATE SCHOOL
December 2018

Approved by: Christopher M. Brophy
Advisor

Robert G. Wright
Co-Advisor

Christopher A. Adams
Second Reader

Garth V. Hobson
Chair, Department of Mechanical and Aerospace Engineering

THIS PAGE INTENTIONALLY LEFT BLANK

ABSTRACT

The emergence of high-performance, consumer-grade, and low-cost drones (under $1000), combined with artificial intelligence and low-cost computer processing power, have provided the tools and platforms on which to build drone swarms. In the context of recent weaponization of commercially available unmanned aerial systems (UAS) such as quadcopters, these trends present two major challenges: the possibility of defenses getting overwhelmed and the large cost asymmetry between currently available defenses and the cost of these threats.

Survivability methodology was used to study the susceptibility and vulnerability of threat vehicles. This analysis was then used to design and develop a submunition possessing a low-cost kill mechanism, so that multiple units could be delivered by a low-cost delivery vehicle. Vulnerability analysis revealed that a fouling mechanism would be highly effective and was therefore chosen as the kill mechanism. The submunition's aerodynamics were modeled and used to develop a concept of operations involving the deployment of multiple submunitions from a single delivery vehicle. The kill mechanism, submunition, and delivery vehicle were manufactured using commercially available components and additive manufacturing. Experimental testing has demonstrated the viability of these designs and the ability to provide a defense against small UAS swarms with low-cost technologies.

THIS PAGE INTENTIONALLY LEFT BLANK

TABLE OF CONTENTS

I. INTRODUCTION....1
A. EMERGING COST ASYMMETRY IN WARFARE....1
B. UNDERSTANDING THE THREAT....2
1. Categorizing Unmanned Aerial Systems....2
2. Autonomy....2
3. Weaponization....3
4. Cost....3
5. Swarm Characteristics....4
C. OBJECTIVES....4

II. THE SURVIVABILITY DISCIPLINE AND METHODOLOGY....7
A. UNDERSTANDING THE KILL CHAIN....7
B. APPROACH AND METHODOLOGY....8
C. DEFINING A REPRESENTATIVE SYSTEM....8
D. DEVELOPING A COUNTER-SWARM WEAPON....10

III. SUSCEPTIBILITY ANALYSIS....11
A. ELECTROMAGNETIC SIGNATURES....12
1. Radio Detection and Ranging (RADAR)....12
2. Infrared (IR)....16
3. Light Detection and Ranging (LIDAR)....18
4. Visual Signature....18
B. ACOUSTIC SIGNATURE....20
C. SENSOR EMPLOYMENT CONCEPT....21

IV. AIRCRAFT VULNERABILITY ANALYSIS....23
A. CRITICAL COMPONENTS AND KILL MODES....23
1. Fault Tree Analysis and Vulnerability Reduction....26
B. VULNERABLE AREA ANALYSIS....29
1. $P_{K|H}$ Determination Using Fragmentation....29
C. KILL MECHANISM ANALYSIS....31
1. Severing Communications Links....31
2. Electromagnetic Energy Exposure (EMP)....31
3. Heat and Blast Exposure (Thermobaric)....32
4. Directed Energy Weapons....32
5. Fouling and Entanglement Obstacles....32
6. PK|H Determination for a Fouling Mechanism....33

V. SUBMUNITIONS AND KILL MECHANISM DEVELOPMENT 35
A. CONCEPT OF OPERATIONS (CONOPS).....35
1. Detection 35
2. Acquisition and Targeting.....35
3. Launch and Delivery.....35
4. Intercept.....36
5. Twin Engagement Scenarios.....36
B. SUBMUNITION DESIGN 38
1. Submunition Aerodynamic Analysis.....38
2. Bomblet Design.....43
C. KILL MECHANISM DESIGN 44
D. DELIVERY VEHICLE.....46

VI. TESTING CAMPAIGN 47
A. KILL MECHANISM TESTING.....47
1. Proof of Concept (First Generation) 47
2. Flight Test Rig (Second Generation).....47
B. BOMBLET TESTING.....51

VII. CONCLUSIONS 55
A. SUMMARY 55
B. FUTURE WORK.....55

APPENDIX.....57

LIST OF REFERENCES.....59

INITIAL DISTRIBUTION LIST 63

LIST OF FIGURES

Figure 1. Kill Chain. Source: [14]. 7

Figure 2. Impedance as a function of index of refraction at a medium interface. 14

Figure 3. Fault tree for attrition kill on a weaponized low-cost commercial UAS. 26

Figure 4. Fault tree for mission kill on a weaponized low-cost commercial UAS. 26

Figure 5. Fault tree for combined mission and attrition kills for a low-cost commercial UAS. 27

Figure 6. Skywalker Technologies X-6 FPV Wing EPO 1500mm. Source: [27]. 29

Figure 7. Engagement geometry. 36

Figure 8. Vertical and horizontal profiles of minimum range intercept. 37

Figure 9. Grid fin modelling in SolidWorks Flow. 40

Figure 10. Lift forces on fin design 41

Figure 11. Drag forces on fin design. 41

Figure 12. Initial submunition design used for SolidWorks Flow analysis. 42

Figure 13. Lift force on submunition body. 42

Figure 14. Drag forces on submunition body. 43

Figure 15. SolidWorks model of bomblet designed by Robert Wright at NPS Rocket Lab 43

Figure 16. Initial kill mechanism design fitted with brass weights and packaged Dyneema net 45

Figure 17. Second kill mechanism design fitted with drop test rig 46

Figure 18. Second kill mechanism with net packaged in stowage space and held with tape. 48

Figure 19. Nose-down deployment test configuration. 49

Figure 20. Flight test rig net firing 1. 49
Figure 21. Flight test rig net firing 2. 50
Figure 22. Flight test rig net firing 3. 50
Figure 23. Flight test rig net firing 4 50
Figure 24. Nose-mounted submunition 51
Figure 25. Nose-mounted submunition on rocket in launch configuration. 52
Figure 26. Servo section with partially deployed fins, remaining on the rocket, as seen from the submunition camera. 53
Figure 27. Front half of the bomblet falling away from rocket as seen by rear-facing camera mounted on rocket. 53
Figure 28. Gouging caused in the submunition stowage tube by the departing bomblet. 54
Figure 29. Bomblet front half debris field at impact location. 54

LIST OF TABLES

Table 1. U.S. DoD classification summary table. Source: [3]. 2

Table 2. Performance goals of a representative threat system. Source: [16]. 9

Table 3. Assessed performance of designed representative threat system. Source: [16]. 10

Table 4. Assumptions made for RADAR range analysis. 15

Table 5. Assessed RADAR detection range results. 15

Table 6. Assessed IR detection range results for frontal profile for various focal lengths and probability of detection. 17

Table 7. Assessed IR detection range results for side profile for various focal lengths and probability of detection. 18

Table 8. Subsystem functional grouping. 23

Table 9. Summary of critical components and assessed kill modes 25

Table 10. Summary of Vulnerability Reduction Principles applied to low-cost UAS. 28

Table 11. Vulnerable Area Determination of the Representative Threat system. 30

Table 12. Engagement scenarios and tactics. 38

Table 13. Submunition terminal velocity determination using SolidWorks Flow. 39

Table 14. Bill of Materials (BOM) for bomblet with approximate costs 44

Table 15. Parts list for representative threat system designed by Capt. Kai Grohe. 57

THIS PAGE INTENTIONALLY LEFT BLANK

LIST OF ACRONYMS AND ABBREVIATIONS

AGL	Above Ground Level
BDA	Battle Damage Assessment
BOM	Bill of Materials
CAD	Computer Aided Design
CONOPS	Concept of Operations
COTS	Commercial-off-the-shelf
CRUSER	Consortium for Robotics and Unmanned Systems Education and Research
DoD	Department of Defense
EM	Electromagnetic
E^3A	Essential Events and Elements Analysis
EMP	Electromagnetic Pulse
FDM	Fused Deposition Modelling
FL	Flight Level
FOV	Field of View
IDF	Israeli Defence Forces
IED	Improvised Explosive Device
IR	Infrared
LIDAR	Light Detection and Ranging
LWIR	Long-Wave Infrared
MAE	Mechanical and Aerospace Engineering
MGTOW	Maximum Gross Take-off Weight
MWIR	Medium-Wave Infrared
NATO	North Atlantic Treaty Organization
NPS	Naval Postgraduate School
RADAR	Radio Detection and Ranging
RCAF	Royal Canadian Air Force
RCS	Radar Cross-Section
sUAS	Small Unmanned Aerial System
SWIR	Short-Wave Infrared

TRADOC	U.S. Army Training and Doctrine Command
UAS	Unmanned Aerial System
USN	United States Navy
X-MADIS	Expeditionary Mobile Aerial Defense Integrated System

ACKNOWLEDGMENTS

I am sincerely grateful for the opportunity rendered to me by the Royal Canadian Air Force to attend the Naval Postgraduate School for over two years in pursuit of a graduate education for my professional development and betterment. My academic endeavors have been made fruitful and enjoyable because of the incredible faculty and staff at NPS. From the staff at the International Graduate Programs Office to the Mechanical and Aerospace Engineering departmental staff (Cdr. Todd Greene, Professor Garth Hobson, and the education technicians), the exceptional support provided has allowed me to pursue academic endeavors beyond what I envisioned at the start of my journey at NPS.

I would like to thank Professor Christopher Brophy, my advisor, and the rest of the staff at the NPS Rocket Lab (Lee Van Houtte, Dave Dausen, and Dr. Josh Codoni) for their support with funding, advice, and labor toward my thesis project. Among the staff at the Rocket Lab, the support of my co-advisor Robert (Bobby) Wright stands out. Bobby has spent countless hours designing and building parts, guiding the various design and testing efforts, and providing technical and academic advice to bring this thesis project to its successful completion. I would also like to thank Professor Christopher Adams, my second reader, for introducing me to the subject of survivability and for the support provided in applying this field of knowledge to this thesis topic. My gratitude also goes to Capt. Kai Grohe (RCAF), on whose thesis work this project was furthered, and fellow students at the NPS Rocket Lab, particularly LT Matthew Busta (USN), without whose shared effort the test launches would not be possible.

The innumerable challenges that must be overcome during a graduate education would be insurmountable without the tremendous support of colleagues, friends, and family. Particular among these were my fellow international students from my refresher quarter and my fellow students in the Mechanical and Space Systems Engineering programs. Above all else, I owe my success to the love and support of a dedicated military spouse and a loving child. Mena and Penny, I share this accomplishment with you.

THIS PAGE INTENTIONALLY LEFT BLANK

I. INTRODUCTION

A. EMERGING COST ASYMMETRY IN WARFARE

Throughout history, combatants have always sought to exploit asymmetric advantages, as a way to maximize damage to their opponents while minimizing harm to themselves. The strategic goal of such warfare is rarely to defeat the enemy's forces in the battlespace [1]. Often, the goal is simply to bleed resources, damage the enemy's morale and to create tactical opportunities. Whereas until recently such attacks have primarily consisted of traditional guerilla warfare, the confluence of various technological developments in the last decade has brought about the advent of a new asymmetric threat: autonomous vehicle swarms.

Several key technologies have converged to make this threat a reality. Swarms of vehicles conducting an attack requires low-cost vehicle platforms, artificial intelligence, and low-cost computer processing power. The emergence of consumer-grade low-cost drones (under $1000) combined with the aforementioned trends has provided the platforms on which to build large drone swarms. The cost asymmetry becomes obvious by solely considering the cost to defeat a single remotely piloted drone. In the most extreme case, the cost to defeat a single threat can exceed the wildest imaginations. In March 2017, Gen. David Perkins, Commander of the U.S. Army Training and Doctrine Command (TRADOC) detailed how the Israeli Defence Forces (IDF) defeated an enemy drone valued at approximately $200 with a Patriot surface-to-air missile with a unit cost greater than $3 million [2]. Extending this incident, it is possible to imagine a scenario where defenses can be easily overwhelmed, from both tactical and economic perspectives. As such, it is incumbent on modern military forces to consider and develop technologies which will be capable of defeating emerging low-cost threats at a cost match or near-match.

B. UNDERSTANDING THE THREAT

1. Categorizing Unmanned Aerial Systems

The U.S. Department of Defense (DoD) broadly categorized unmanned aerial systems (UAS) into five groups based on maximum gross take-off weight (MGTOW), nominal operating altitude, and nominal operating speed [3] as detailed in Table 1.

Table 1. U.S. DoD classification summary table. Source: [3].

<table>
<tr><th>UAS Group</th><th>Maximum Gross Take-off Weight (MGTOW) (kg)</th><th>Nominal Operating Altitude (m)</th><th>Speed (m/s)</th><th>Representative UAS</th></tr>
<tr><td>Group 1</td><td>0 – 9</td><td>< 366 AGL</td><td>< 51</td><td>RQ-11 Raven</td></tr>
<tr><td>Group 2</td><td>9.5 - 25</td><td>< 1067 AGL</td><td rowspan="2">< 129</td><td>ScanEagle</td></tr>
<tr><td>Group 3</td><td>< 599</td><td rowspan="2">< FL 180</td><td>RQ-7B Shadow</td></tr>
<tr><td>Group 4</td><td rowspan="2">> 599</td><td rowspan="2">Any airspeed</td><td>MQ-8B Fire Scout
MQ-1A/B Predator</td></tr>
<tr><td>Group 5</td><td>> FL 180</td><td>MQ-9 Reaper
RQ-4 Global Hawk</td></tr>
</table>

Low-cost systems generally fall into Group 1 or Group 2. However, even systems in these categories can carry tactically relevant payloads. For example, the DJI MG-1 AGRAS is an agricultural spraying drone, and can carry and disperse 10 kg of liquids [4] and retails for approximately $15,000. Conversely, at the opposite end of the cost spectrum, are drones like the Syma X-8C. This is a drone that retails for approximately $100 and can carry a payload of 0.2 kg. This equates to half the weight of an M67 fragmentation grenade. Fixed wing drones, ranging in price from a few hundred to several thousand dollars, with capabilities including advanced sensors or aerial spraying are also emerging from the agricultural community [5].

2. Autonomy

Autonomy can range from single features to swarm control. At the most basic level, commercially available drones can be programmed to follow pre-determined paths

and execute pre-determined actions, employing onboard sensors, (such as GPS receivers, IR, stereovision, etc.) and inertial navigation systems (INS) which normally incorporate a compass, accelerometers and gyroscopes.

In December 2017, China put on a record setting aerial display using 1,180 drones to exhibit an aerial light show as part of the welcoming ceremony for the Guangzhou Fortune Forum. The exhibit was controlled by a single console and operator, developed by Chinese start-up eHang [6] using commercially available technologies with some of their own innovations. In July 2018, Intel conducted a similar demonstration with 500 drones, at Travis AFB, for Independence Day celebrations [7].

The evolution of artificial intelligence, will, in due course, enable an extremely high level of autonomy. A demonstration of a high level of autonomy, while operating as a swarm, was shown by DoD's Strategic Capabilities Office. The drone swarm demonstrated "collective decision-making, adaptive formation flying and swarm self-healing." [8] The Perdix drones used for the demonstration were 16.5 cm (6.5") in length, 30 cm (11.8") in wingspan, with 6.6 cm (2.6") propellers, weighing 290g [9].

3. Weaponization

Commercially available quadcopters are already being employed by various opposing forces in Iraq and Afghanistan. In early 2017, reports emerged of the Islamic State in Iraq and Syria (ISIS) using quadcopters to drop various explosive devices, from grenades and IEDs to fused mortar rounds [10]. These videos show drone operators engaging in careful target selection (with a preference for lightly armored vehicles), descent to a release point, and post-release egress maneuvers and camera slewing for possible Battle Damage Assessments (BDA). These videos offer evidence that weaponization of commercially available quadcopters is becoming regularized as an option for asymmetric warfare.

4. Cost

The costs of a drone can vary substantially according to capability. There is, however, some consistency in the relative pricing of components. The major cost drivers

for drones are often the "brains" of the system, or the chipsets used to control the vehicle, communicate with other vehicles, maneuver and exercise collective decision-making. These include the microcontroller chipsets, onboard sensors, communications systems and motors [11]. With development of artificial intelligence chipsets, largely driven by commercial information technology requirements, it is predicted that costs of these chipsets can be driven down to $25 by 2022 [12]. Structural components and batteries are relatively cheap. And in the case of drones developed without re-use considerations, the costs for the latter components can be even lower.

5. Swarm Characteristics

With increasing autonomous capabilities, UAS swarms are adapting certain characteristics of resilient systems, in response to disruptions [13]:

- heterogeneity—the uniformity of response to a specific disruption
- modularity—the ability of the swarm to compartmentalize sub-elements; and
- randomness—the predictability of the response to a given disruption.

Resilient systems demonstrate these qualities in response to disruptive events. These events can range from systemic, external or human-triggered. The range and quality of response can be used to characterize the level of resilience, itself a proxy measure of autonomy.

C. OBJECTIVES

Defeating future swarm threats at costs approaching parity requires the design and development of several key technologies at relatively low cost. The objectives of this research project are to:

- analyze and assess a representative threat system using an appropriate methodology to inform the development of systems that could counter small UAS (sUAS) swarms;

- develop a delivery system consisting of a single platform or employing a collection of submunitions, capable of intercepting multiple targets in a swarm;
- design a conceptual framework for the employment of these counter-UAS systems against a swarm; and,
- develop a compact terminal defeat mechanism for sUAS that can be employed in conjunction with the delivery system to neutralize the platforms being employed in the swarm.

Reducing cost asymmetry will require that these systems use commercial-off-the-shelf (COTS) components and non-specialized, commercially available fabrication techniques. As such, these technologies need to be designed and developed using software and tooling regularly available at NPS.

THIS PAGE INTENTIONALLY LEFT BLANK

II. THE SURVIVABILITY DISCIPLINE AND METHODOLOGY

A. UNDERSTANDING THE KILL CHAIN

Weapon systems achieve a mission kill (failure of the threat system to achieve its objectives) or attrition kill (destruction or incapacitation of the threat system) through a sequence of events known as the kill chain. This kill chain, as depicted in Figure 1, is the product of the probabilities of those events.

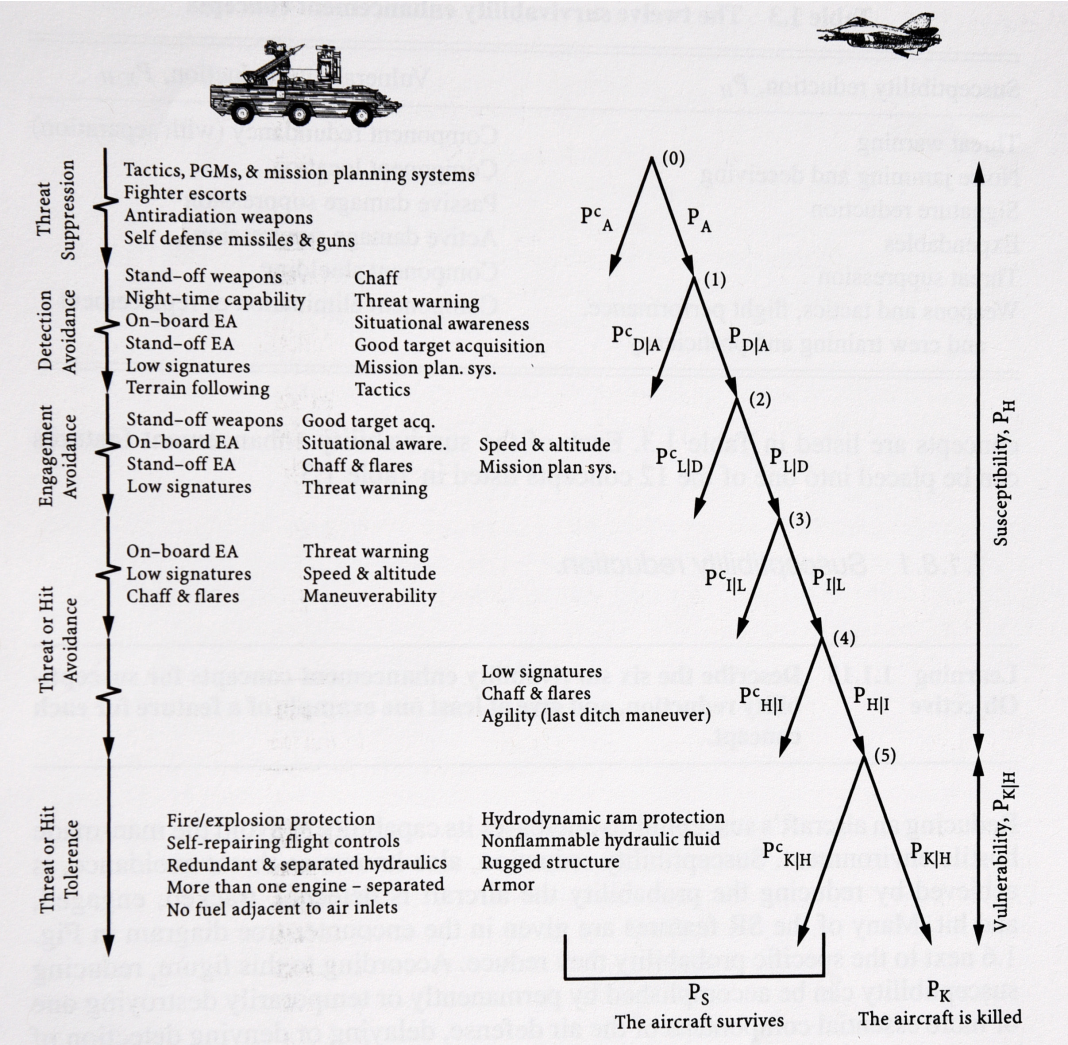

A successful kill requires success on a chain of events, which have individual probabilities. These combine to form a "Kill Chain."

Figure 1. Kill Chain. Source: [14].

The probability of an incoming threat UAS being killed is a function of the readiness of the air defence system, detection of the UAS, successful engagement by defensive countermeasures or weapons and damage from an engagement:

$$P_K = P_A \cdot P_{D|A} \cdot P_{L|D} \cdot P_{I|L} \cdot P_{H|I} \cdot P_{K|H} \quad (1)$$

A successful defensive engagement requires all components of the kill chain to have a high probability of success. When designing a weapon system, designers have some control over the detection, intercept, hit and kill phases of the kill chain. The remaining phases are operationally defined. Optimization of the kill chain requires analysis of both the threat and response systems over these design phases.

B. APPROACH AND METHODOLOGY

The Survivability Discipline, significantly codified by Robert E. Ball in *The Fundamentals of Aircraft Combat Survivability Analysis and Design* [14], can essentially be applied by considering two major subordinate fields of study: susceptibility and vulnerability. Susceptibility is concerned with the likelihood of the platform being successfully targeted and hit by a weapon (expressed as the Probability of Hit (P_H)). Vulnerability is concerned with the likelihood of the platform being immobilized or destroyed or degraded (to a point of negating it as a threat), following impact by a weapon (expressed as the Probability of Kill given a Hit ($P_{K|H}$). The product of these two analyses will provide the likelihood of a target being killed:

$$P_K = P_H \cdot P_{K|H} \quad (2)$$

To assess the likelihood of a successful kill chain, analysts normally combine a susceptibility analysis and a vulnerability analysis. This methodology can be used to develop a system that will be successful in engaging and eliminating small UAS threats.

C. DEFINING A REPRESENTATIVE SYSTEM

Development of a low-cost counter-swarm weapon requires the study of a representative threat system. As detailed earlier, a representative threat system would be a low-cost system capable of lethal swarm attacks.

The development of a system with such performance characteristics can be accomplished using commercial-off-the-shelf components with instructions from hobbyist websites. The instructables.com website offers guidance for hobbyists on building drones with a list of design steps (first 6 of 20 steps) [15] :

1. Find a purpose for your aircraft.
2. Pick your electronics.
3. Estimate the total weight of your aircraft.
4. Determine wing loading.
5. Decide on a wingspan.
6. Design your fuselage and tail section.

Applying the steps to the design of a small self-designed drone, the outline of a self-designed drone can be defined. The target performance criteria, listed in Table 2, were defined as:

Table 2. Performance goals of a representative threat system. Source: [16].

Performance Criteria	**Desired value**
Velocity	20 m/s
Payload	2-3 kg
Endurance	20-60 mins
Unit Cost	< $1000

The goal of the criteria in Table 2, was to define a small UAS capable of delivering a payload with a similar weight to that of a fragmentation or High Explosive Anti-Tank warhead employed with an RPG-7. Following these steps, a representative aircraft was defined with a parts list and appears in the Appendix. Analysis of the above system, by Capt. Kai Grohe (Royal Canadian Air Force (RCAF)), using various online

hobbyist calculators and basic aerodynamics calculations predicted performance, is listed in Table 3.

Table 3. Assessed performance of designed representative threat system. Source: [16].

Performance Criteria	Predicted Value
Velocity	23.3 m/s
Payload	1.9 kg
Endurance	20 mins
Estimated cost	< $1000 / unit

This defined system represents a threat that could be employed at low-cost in a swarm configuration to overwhelm potential defenses. Assessing the survivability characteristics of such a system will allow for the definition of potential kill mechanisms.

D. DEVELOPING A COUNTER-SWARM WEAPON

This report will use the methodology laid out by Dr. Ball to perform a susceptibility analysis (Chapter III) and vulnerability analysis (Chapter IV) on the representative threat system, and other sUAS. These analyses rely on literature surveys of existing technologies, applied to the problem of countering small UAS threats.

These analyses will then be used to design a submunition and a kill mechanism, and to develop a concept of operations to deploy these systems against the representative threat (Chapter V), using an existing low-cost delivery vehicle. Test campaign results will be detailed in Chapter VI.

III. SUSCEPTIBILITY ANALYSIS

Susceptibility refers to "the probability of a platform being impacted by one or more damage/kill mechanisms in the pursuit of its mission." [14] The susceptibility of a platform in an encounter with a countering system is dependent upon three factors: the performance and lethality of the countering system, the characteristics of the platform itself and the engagement scenario. From the kill chain, susceptibility (defined as Probability of Hit (P_H)) is a combination of several factors captured in the susceptibility equation:

$$P_H = P_A \cdot P_{D|A} \cdot P_{L|D} \cdot P_{I|L} \cdot P_{H|I} \quad (3)$$

where,

- P_A is the probability that the defensive system is active;
- $P_{D|A}$ is the probability that the defensive system detects the threat;
- $P_{L|D}$ is the probability that the defensive system launches a countermeasure weapon against the threat;
- $P_{I|L}$ is the probability of an intercept given a launched countermeasure; and,
- $P_{H|I}$ is the probability of a hit by the countermeasure weapon given an intercept trajectory.

All of these factors are largely dependent on the engagement scenario including the operational posture and tactics employed by the defensive system at the time of engagement. The greatest variability, which can be qualitatively assessed using open source literature, is the probability of detection ($P_{D|A}$). As such, a threat platform susceptibility assessment based on the signatures of commercially available drones could inform on the detectability of a threat UAS.

A susceptibility assessment is "a modelling and quantification of the sequence of events and elements in the encounter between the aircraft and the threat against it, until one or more hits on the aircraft occurs." [14] Normally referred to as an "Essential Events and Elements Analysis" (E^3A). An effective susceptibility study would consider the platform's observables or detectable signatures, aerodynamic performance and self-protection capabilities. Scenario modeling would normally include the physical environment in which the encounter occurs, multi-platform deployment patterns and activity including flight paths, tactics and any supporting forces. With low-cost small UAS systems as detailed in the representative threat system, the susceptibility assessment must necessarily focus on observability. Swarms employing low-cost UAS are unlikely to employ self-protection measures on individual platforms due to cost considerations, and aircraft size and performance limitations. The swarm would likely rely on large numbers overcome the disadvantage of reduced self-protection.

One of the key events in susceptibility assessments is the probability of detection ($P_{D|A}$) which depends heavily on the aircraft's signature. The lower the aircraft signature, the lower the probability of detection and hence lower probability of kill (i.e., lower susceptibility). There are several signatures that could be considered including those across the electromagnetic (EM) spectrum, and aural signature. Quantitative assessments would be challenging given the breadth of the field and the paucity of granular data. However, it is possible to do a qualitative assessment on the different signatures and consider a conceptual framework for the employment of sensors to maximize the probability of detection.

A. ELECTROMAGNETIC SIGNATURES

The electromagnetic emissions of a target can range from active transmissions to reflections of energy across the electromagnetic spectrum, including in the radio, infrared and visible light portions of the spectrum.

1. Radio Detection and Ranging (RADAR)

Radar is an object-detection system that uses radio waves to detect, identify and classify objects. Radar antennas radiate EM pulses in the direction of the target. When the

signal passes over the target, some of the incident energy in the EM pulse is absorbed as heat, some is reflected, and some passes through the material it contacts. The ability of the radar to detect the target depends on energy that is reflected or re-radiated from the target back toward the radar receiver.

There are two schemes of radar operation: active and semi-active. Active radars rely on co-located transmitters and receivers to detect and triangulate a threat's position. Semi-active radars combine, either an off-board transmitter or a transmitter located separately on the weapon, which illuminates the target, with on-board receivers which only receive the signals. The range of detection is governed by the radar range equation:

$$R_{Max} = \left[\frac{P\ G^2\ \lambda^2\ \sigma}{(4\pi)^3\ N\ SNR}\right]^{1/4} \quad (4)$$

where,

- P is the peak output power;
- G is the antenna gain;
- λ is the wavelength;
- σ is the Radar Cross-Section (RCS);
- N is the noise power; and,
- SNR is the minimum signal to noise ratio.

The variables in the equation change depending on the environment and equipment involved. The amount of energy returned is highly dependent on the radar cross section (RCS) of the target. The RCS is a function of absolute size, material, incident angle, and reflected angle. Two of these are a function of the aircraft's design and can be studied using approximate characteristics of the representative threat:

- Size. The representative threat UAS is assumed to have a length of 1m and a wingspan of 1.5m and a side profile height of 0.25m.

- Material. The representative UAS is presumed to have wings made of a light-weight foam material which has a relative permittivity (ε_r) and permeability (μ_r) of approximately 1.0. This is the approximate impedance of air. Since foam and air are fairly close in impedance, there is likely to be very little reflection or re-radiation of the electromagnetic wave from the target. This is shown in Figure 2, where the surface reflectance is zero when the impedance of the target is equal or close to the impedance of air. Hence, the material of the UAS is considered 'radar absorbent' and very little energy is reflected back to the radar which makes it very hard to detect.

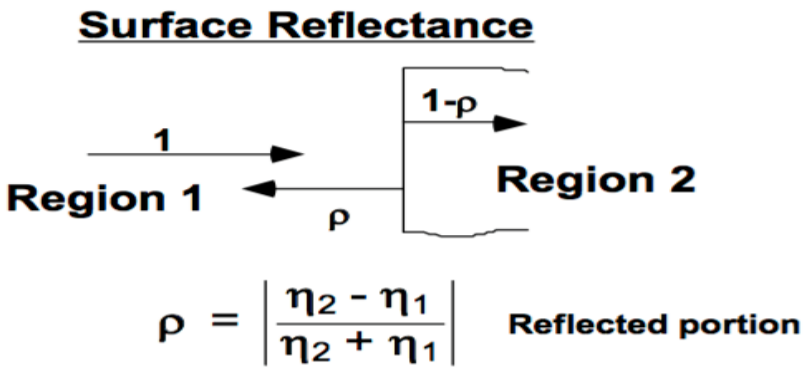

Figure 2. Impedance as a function of index of refraction at a medium interface.

Due to their small size and the common use of radar absorbent material, low-cost UAS often have small RCS/ radar signature and are therefore, difficult for any radar to detect at ranges that would be tactically useful. For example, experimental results obtained by C. J. Li and H. Ling for the RCS measurements of three popular commercially available quadcopters (DJI Phantom 2, DJI Inspire 1 and 3DR Solo) varied from -9.3 dBsm to -19.4 dBsm in the 12–15 GHz frequency band depending on the angle of incidence and surface area presented by these drones. The authors note no significant

change in signature with spinning blades and a reduction in the range of 10–11.6 dB in the 3–6 GHz band [17].

Using this data and several assumptions for the radar range equation, a basic estimate of detection ranges can be constructed for an active system on board. These assumptions, detailed in Table 4, were based on work done during the ME4704 Missile Design course, with input from Dr. David Jenn at NPS.

Table 4. Assumptions made for RADAR range analysis.

Radar Characteristic	Assumed Specification
Transmitted Power	5W
Antenna Diameter (Missile)	17.78 cm (7”)
Antenna Diameter (Ground)	60.96 cm (24”)
Antenna Efficiency	0.7
Frequency	13.5 GHz
Signal-to-Noise Ratio (SNR)	15 dB
Bandwidth	100 MHz
Equivalent Noise Temperature	290 K

Using these assumptions, the gains for the semi-active and active antennas (missile and ground were) were calculated:

$$G = \frac{4\pi Ae}{\lambda^2} \tag{5}$$

These gains were then used with the radar range equation to determine the maximum detection ranges using the radar cross sections provided by Li and Ling. The results for an onboard active radar, ground based active radar and a semi-active radar employing a ground-based transmitter and an aerial receiver are presented in Table 5.

Table 5. Assessed RADAR detection range results.

RCS	Active (Airborne)	Active (Ground Based)	Semi-Active
-19.4 dBsm	0.121 km	1.57 km	0.88 km
-9.3 dBsm	0.218 km	2.81 km	1.57 km

These results demonstrate the challenges with employing radars for detecting and targeting small commercial UAS. Effective detection ranges require higher power ground based active radars. However, even these can be negated with efforts aimed at reducing the radar cross section. This can range from using low impedance materials to flight profiles which minimize the cross-section presented.

2. Infrared (IR)

IR signature is composed of radiation emitted and reflected from the aircraft typically in the 1 to 3 μm (Short Wave Infrared band [SWIR]), 3 to 5 μm (Medium Wave Infrared band [MWIR]) and 8 to 12 μm (Long Wave Infrared band [LWIR]). The general sources of this signature are:

- radiation emitted by the airframe and propulsion system,
- radiation emitted by the exhaust gas or plume from the engine and
- reflected radiation incident on the aircraft.

Relative to a typical aircraft, a low-cost UAS has an extremely low infrared signature. Especially if propelled by a non-combusting propulsion system (electric motors). Aside from the magnitude of the emission, the spectrum also determines which sensors can be most effective at detecting a UAS. Research from the Naval Air Weapons Centre indicates that sensors in the MWIR region are most effective at picking up emissions such as reflected sunlight [18]. Zheng et al. also found that the peak spectral intensity for UAS using a turbine occurred in the Medium Wave IR range [19]. Sensors using focal plane arrays consisting Mercury Cadmium Telluride (HgCdTe) or Indium Antimonide (InSb) photovoltaic detectors would offer high detectivity for the mid-wave IR spectrum. Compact commercial systems that could be placed onboard an airborne platform or surface surveillance system are available. These systems, however, come at a high cost. An example of such a system is the Zafiro HD Cooled Camera Module by Leonardo DRS Technologies with a spectral response of 3.7 to 5.1 microns [20]. To translate this into an effective probability of detection and range, criteria developed by

John Johnson, translated into equations by John Love from DRS Technologies, was used [21]:

$$Target\ Critical\ Dimension\ (m)\ = \sqrt{Target\ Height\ (m)\ * Target\ Width\ (m)} \quad (6)$$

$$Pixel\ Instantaneous\ FOV\ (mrad) = \frac{detector\ pixel\ pitch\ (\mu m)}{optics\ effective\ focal\ length\ (mm)} \quad (7)$$

$$Pixels\ per\ meter\ Required\ in\ Target\ Plane\ (PPM) = \frac{(2 * \text{No.}\ of\ cycles\ required\ \text{per Johnson criteria})}{Target\ Critical\ Dimension} \quad (8)$$

$$Range\ (m) = \frac{1000\frac{mrad}{rad}}{PPM * Pixel\ Instantaneous\ FOV} \quad (9)$$

Using these equations and assuming a detector pixel pitch of 12 μm, with the number of cycles in the Johnson criteria as 0.75 for 50% probability of detection and 1.34 for 90% probability, yields the following detection ranges for the representative threat, with a maximum presented area of 1.5m by 1m.

Table 6. Assessed IR detection range results for frontal profile for various focal lengths and probability of detection.

Focal Length	FOV	Maximum Detection Range (50%)	Maximum Detection Range (90%)
28 mm	30.7°	1.80 km	1 km
65 mm	13.5°	4.16 km	2.33 km

However, when considering a minimum presented area (side profile), approximated by a profile of 1m by 0.25m, detection ranges drop considerably, as seen in Table 7.

Table 7. Assessed IR detection range results for side profile for various focal lengths and probability of detection.

Focal Length	FOV	Maximum Detection Range (50%)	Maximum Detection Range (90%)
28 mm	30.7°	0.73 km	0.41 km
65 mm	13.5°	1.70 km	0.95 km

The range of detection in the case of IR sensors is largely a function of the size of the focal plane array and the trade between focal length and field of view. Larger arrays with finer pixel sizes, increase both the range and the probability of detection. And longer focal lengths increase the range of detection while reducing the field of view.

3. Light Detection and Ranging (LIDAR)

Light detection and ranging systems are active emitting systems which combine the benefits of passive infrared red system with active illumination of the target to boost detectability. These systems use lasers emitting in the SWIR range, with similar arrays to IR receivers. Expected detection ranges should exceed those for passive IR systems as a minimum, with signal gains for combined SWIR LIDAR and passive MWIR, rising up to 30 dB [22]. Such gains can overcome significant limitations with passive systems such as responses at range, during periods of inclement weather or where the threat UAS may be using coatings to minimize reflections. Commercial systems, such as the OPAL 3D LiDAR developed by Neptec Technologies, claim ranges up to 1000m [23].

4. Visual Signature

The visual detectability of a target is dependent on various factors, including its size and the contrast presented between the background and the target. The ability to visually detect an object can be simply summarized by the visual acuity of the observer:

$$d = \frac{w}{\theta} \tag{10}$$

where,

- d is the distance from the object to the observer;
- w is the width of the object; and,
- θ is the visual angle in radians

Average visual acuity is broadly 1 arcminute for most humans (commonly referred to as "20/20 vision"). As such, for a target with a profile diameter of 1m, the maximum distance at which the target can be discerned would be approximately 3448m. However, this theoretical limit is substantially reduced in reality by atmospheric effects, lighting, target shape, relative contrast against the background, position in the human observer's field of view and relative motion [24] [25]. For example, Lappin et al. note that visual acuity for moving objects was limited below 0.5°/s - 1°/s for observers employing peripheral vision or low vision observers. Under such conditions where visual acuity worsens to 5 arcminutes, the range of sight would decrease to 688m for a 1m diameter target. Designs employing smaller visual profiles and lower contrast paint schemes coupled with flight profiles which minimize visual signatures, it can be concluded, would limit a human observer's ability to effectively detect and discern a threat UAS at significant ranges. Moreover, detection can degrade to virtually negligible in low-light conditions.

Electro-optical systems employing optical sensors and computer vision can overcome many of these limitations. Recently fielded systems offer insight into the performance of such systems. The CM202U Gimbal electro-optical turret is a system that is integrated with the X-MADIS (Mobile Air Defense Integrated System), developed by Ascent Vision, for the U.S. Marine Corps. The system asserts a detection range for UAS based on size and motion of 2–3 km, with the ability to identify and classify small multicopters at up to 382m [26]. These passive systems can have their performance substantially improved through supplementation with IR or LIDAR systems.

B. ACOUSTIC SIGNATURE

Aside from electromagnetic signatures, aircraft can also emit noise that would impact their detectability. The acoustic signatures of sUAS offer substantial potential for detectability. Acoustic sensors are composed of passive sensors, usually arrays of microphones, which can be deployed to detect the minute mechanical displacements of air caused by pressure variations from rotating, oscillating or vibrating bodies. For most small, commercial UAS this would be the propeller or rotors used to propel or lift the aircraft [25]. Acoustic sensing has advantages over exploitation of the electromagnetic spectrum. Acoustic sensors are passive, not dependent on ambient light (making them insensitive to diurnal variations) and are typically omnidirectional allowing for the attainment of complete spherical sensing coverage to be achieved [25].

Research conducted on the acoustic detection of small commercial UAS indicates an approximate range of detection of approximately 600m. Harvey and O'Young's research at the Memorial University of Newfoundland employed a Delta X-8, a small electrically powered drone equipped with acoustic sensors mounted on vibration absorbing mounts, to attempt detection of a gasoline fueled, single engine, 1.5m wingspan, fixed wing drone [25]. They employed three methods. The "single trial method" resulted in the longest absolute maximum detection range of 678m with a mean maximum detection range of 302 m. This method also resulted in a 63% false detection rate. The other two methods were forms of binary integration which reduced the false detection rate to under 1%, but also reduced the absolute maximum detection range to 593m and the mean maximum detection range to 258m [25].

Research was conducted by the U.S. Army Research Lab using man-portable arrays. Employing algorithms and filtering to discount false detections, the tetrahedral array employed achieved a 99% probability of detection, at ranges up to 600m, with a 3% false detection rate [26]. However, the researchers also noted that their tests were impacted by other aircraft and that acoustic sensing was unlikely to fare well in a populated environment with several UAS operating at similar frequencies. Interference could result in rendering the signals incoherent resulting in difficulties tracking the UAS [26].

C. SENSOR EMPLOYMENT CONCEPT

To boost the probability of detection, sensors have to be employed in a manner that favors maximum detection. However, there remain various other factors that drive design of the sensor employment concept:

- *Cost.* Sensors with sufficient resolution to effectively target a small UAS through environmental clutter would be expensive.
- *Processing power.* Smaller packaged weapons or submunitions have limits to how much processing power and battery power can be placed onboard, owing to space and thermal considerations.
- *Capability.* Smaller weapon or submunitions are limited by antenna or the size of the sensor window. By contrast, the nose cone of a missile, or its body, has substantially more space for a larger sensor unit. This would allow a larger single sensor or the placement of multiple sensors in the sensor window, or longer and multiple antennas.

These factors drive the selection of a sensor employment concept that chooses between distributing sensors on individual kill vehicles, investing in larger sensors on the ground or a single centralized airborne platform that could guide several kill vehicles through to a successful intercept, (e.g., a "targeting hub'). Centralized sensors are preferred largely because of their favorability on these factors. Centralized sensors, by virtue of fewer restrictions on size can offer higher capability, greater processing power, and the opportunity to limit costs by concentrating investment into fewer large sensors.

Fewer sensors also allows for layering and combination of various sensor systems into networks to maximize detection under various conditions (lighting, weather, terrain, distribution, etc.). The combination of fixed or mobile radars with portable passive electro-optical/IR sensors or LIDARs allows for maximum detection of small UAS swarms. To effectively target small UAS with individual submunitions while considering these factors, it is suggested that a targeting hub positioned over the engagement area would be most suited to intercept a small swarm of low-cost UAS. The small size of

commercial UAS and the materials used to construct them suggest that a LIDAR or MWIR system onboard would be able to take advantage of secondary emissions from these aircraft.

IV. AIRCRAFT VULNERABILITY ANALYSIS

Vulnerability concerns the likelihood of a platform surviving an impact from a kill mechanism designed to destroy the platform itself or impede its function [14]. In the survivability equation, vulnerability is denoted as $P_{K|H}$. To assess vulnerability, a fault tree analysis and a vulnerable area assessment can be employed (as prescribed by Dr. Ball). A fault tree analysis lays out the kill chain of critical subsystems which, if broken, would render the system vulnerable to an attrition kill [14]. In order to determine a numerical value for vulnerability, a vulnerable area assessment can be employed.

A. CRITICAL COMPONENTS AND KILL MODES

The subsystems of a UAS can be grouped into two functional groups, detailed in Table 8, with one group encompassing all systems essential to flight and a second group essential to the performance of the mission.

Table 8. Subsystem functional grouping.

Flight Essential Functions	Mission Essential Functions
Aerostructure Control Systems Propulsion Battery Communications links	Weaponized Payload Video or data links Targeting systems

These subsystems have specific technical or functional vulnerabilities, summarized in Table 9, which represent kill modes that can be used to effect the failure of flight (resulting in an attrition kill) or mission (representing a mission kill):

- *Aerostructure*. Most low-cost commercial UAS are made of low-density materials, with the outer structure bearing very limited aerodynamic loading. As such, low grain kinetic impacts are unlikely to result in catastrophic failure of the aerostructure. Instead, the likely outcome is a steady degradation of lift generation, resulting in deterioration of aircraft

manoeuvrability, altitude sustainment and speed sustainment. In further analysis, the aerostructure is treated as less critical and considered as the total area against which other critical areas were measured.

- *Control Systems*. The Control Systems functions are accomplished by various subsystems including the guidance and navigation systems, flight control surfaces and their actuators, and processor systems for autonomous operations and flight control. Damage that substantially degrades or destroys any of these subs-systems is likely to lead to an attrition kill through a loss of control of the aircraft.

- *Battery*. Power for low-cost drones is most often provided by a battery. The battery group usually consists of a battery and its connections to the motors. On more sophisticated aircraft, there may be additional electronics which provide thermal management of the battery. Interruption of power, either by cutting the battery link to the motor or by damage or destruction of the battery will result in an immediate attrition kill through loss of thrust and/or loss of control of the aircraft.

- *Propulsion*. The propulsion group usually includes the electric motor, driveshaft and propeller. Most of these components are not redundant. And damage to any of these components will result in loss of thrust and a subsequent attrition kill.

- *Communications, Video and Data Links*. Backhaul communications links may be required for control of the aircraft or to initiate payload release or counter enemy defensive actions. Severing communications links will only result in an attrition kill if the aircraft is wholly dependent on remote control for direction. Aircraft can however, be outfitted and programmed to operate autonomously. This would render any loss of communications less relevant. Severing communications links could result in an attrition kill, but a mission kill is far more likely. In the event that the aircraft is

fully autonomous though, loss of communications is unlikely to have any impact on the aircraft. This assessment consider the likelihood for full autonomy high and therefore disregards communications links from further consideration as a critical component.

- *Weaponized Payload*. The payload represents a large surface area for the aircraft. It is also the most volatile of the critical components. Significant damage could result in deflagration of the payload, resulting in immediate destruction of the aircraft. Mission failure could also be incurred by preventing a successful deployment or fusing of the payload.

- *Targeting Systems*. Depending on the platform, this could range from some kind of seeker to a proximity fuse. Damage or destruction of this subsystem may result in a mission kill. An attrition kill is unlikely.

Table 9. Summary of critical components and assessed kill modes

Critical Components	**Assessed Kill Modes**
Aerostructure	Loss of Lift Structural compromise or failure
Control Systems	Autonomous and flight control systems processors Actuator Failure Flight Control Surface damage or failure Guidance systems failure
Battery	Battery Disconnection Catastrophic battery failure (puncture, fire, thermal runaway)
Propulsion	Propeller/drive shaft failure Electric Motor failure
Communications Links / Video or Data Links	Loss of video or sensor feed Loss of backhaul communications links
Weaponized Payload	Release separation failure Trigger/fuse failure Deflagration of the warhead/payload
Targeting Systems	Sensor failure Data processor failure

1. Fault Tree Analysis and Vulnerability Reduction

Considering systems vital to the flight and mission functions of the aircraft which represent critical systems, this is the fault tree (shown in Figure 3) that can be generated for an attrition kill.

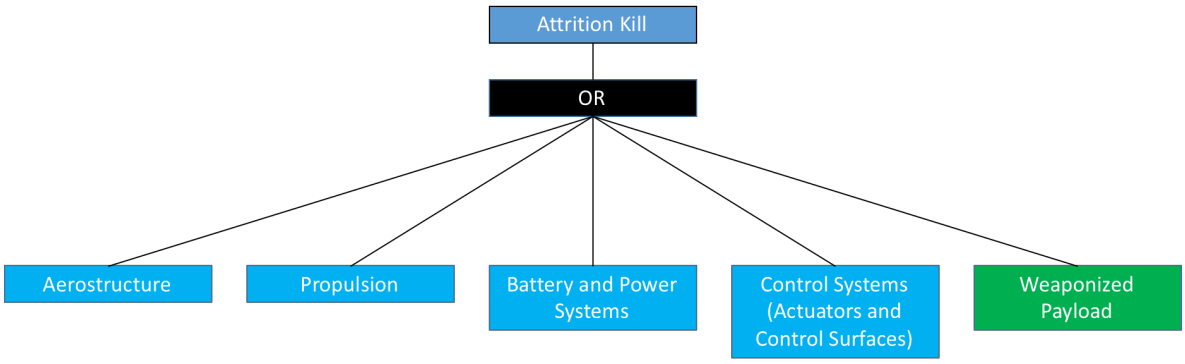

Figure 3. Fault tree for attrition kill on a weaponized low-cost commercial UAS.

Similarly, considering systems essential to the performance of the mission by not necessarily required for they systems operations, the mission kill tree (depicted in Figure 4), can be generated.

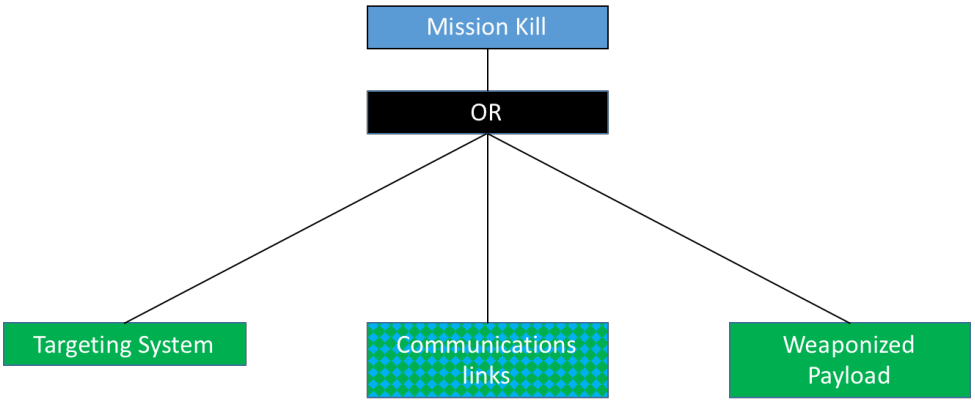

Figure 4. Fault tree for mission kill on a weaponized low-cost commercial UAS.

Combining the fault trees in Figure 3 and Figure 4 leads to the kill tree shown in Figure 5:

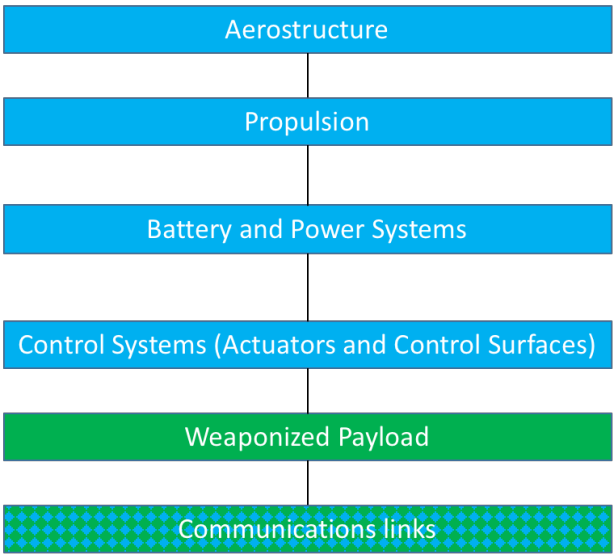

Figure 5. Fault tree for combined mission and attrition kills for a low-cost commercial UAS.

From the Figure 5, it is clear that sUAS do not observe the several Vulnerability Reduction principles as detailed by Dr. Ball, and summarized in Table 10. There are various approaches that can be used to provide some reduction in vulnerability to an encounter with a threat to the platform [14]:

- *Component Redundancy*. The small size of commercial UAS airframes, and the low-cost limit does not allow for the employment of redundant systems. Incorporating redundancy, would require dramatic increases in cost, while increasing both vulnerable areas and possibly the overall size of the aircraft.

- *Component Location*. This principle may be employed. And the most likely method would be the placement of system components such that that their vulnerable area is reduced in the largest presented profile (the planform profile).

- *Passive and Active Damage Suppression.* Cost prohibitions and space limitation severely limit the ability to employ damage suppression techniques or technologies. Low-cost UAS often use commercial-off-the-shelf components. As such, damage and ballistic tolerance are unlikely to incorporated. Active suppression systems such as fire suppression bottles are also unlikely for size, cost and complexity reasons.

- *Component Shielding*. As with some of the other principles, cost, complexity and size considerations reduce the likelihood that components will be adequately shielded. Additionally, the aircraft will have a limited payload. Shielding would reduce payload capability, reducing the effectiveness of the platform.

- *Component Elimination or Replacement*. This principle is likely to be employed, simply through technological advancements. Electronics packages that fulfil multiple functions could result in component elimination or replacement with smaller or more effectively shaped components, reducing the net vulnerable area.

Table 10. Summary of Vulnerability Reduction Principles applied to low-cost UAS.

Vulnerability Reduction Principle	Applied?
Component Redundancy	No
Component Location	Yes
Passive Damage Suppression	No
Active Damage Suppression	No
Component Shielding	No
Component Elimination or Replacement	Yes

B. VULNERABLE AREA ANALYSIS

1. $P_{K|H}$ Determination Using Fragmentation

To assess the probability of kill of a low-cost commercial UAS against a fragmentation warhead, the components of the representative threat system were used with approximate dimensions to model vulnerable areas compared to a triangular planform. This planform was based on the Skywalker Technologies X-6 FPV Wing shown in Figure 6.

Figure 6. Skywalker Technologies X-6 FPV Wing EPO 1500mm. Source: [27].

This analysis includes some assumptions:

- Aerostructure was not considered a critical component and provided the baseline presented area. Fragments can penetrate and damage the aerostructures (usually made of foam) without causing failure.
- Components were placed such that they maximized their presented area on the planform profile.
- The side profile was assumed to have a low of probability of hit and not assessed for $P_{K|H}$.

These assumptions lead to the estimation of vulnerable areas, detailed in Table 11.

Table 11. Vulnerable Area Determination of the Representative Threat system.

Component	L (mm)	W (mm)	Presented Area (A_P) (m^2)
Motor	50	55	0.00275
Propeller	13	12	0.000156
Battery	168	69	0.011592
Controller	45	24	0.00108
Guidance	43.18	38.1	0.00164516
Servos (4)	75	75	0.0225
Warhead (based on 2kg RPG-7 Frag)	317	40	0.01268
Total Vulnerable Area (A_V)			**0.05240316**
Flying Wing Body (Aerostructure) (A_P) L*W*0.75	660	1500	**0.7425**

Comparing the vulnerable area against the planform of the aerostructure provided for a determination of probability of kill given hit (single shot or fragment):

$$P_{K|H} = \frac{A_V}{A_P} = \frac{0.05240}{0.7425} \approx 0.071 \quad (10)$$

The probability of a fragment impact on a critical area could be increased by increasing the aereal density of the fragments. However, the scaling of the fragment spray area scales geometrically as radius increases if only the sidewalls of a cylindrical warhead are considered:

$$A_{side\ spray} = 2\pi rh \quad (11)$$

Therefore, simply doubling the radius results in a 50% reduction in the aereal density of fragments. Therefore, a fragmentation warhead would have to be fused relatively close to the target. At approximately 14r, the aereal density approaches that of the probability of kill given hit. Given the size of most compact warheads, this would imply a minimum fusing distance of substantially less than 10m to achieve an increase in the probability of a fragment successfully striking a vulnerable area.

The low probability of kill given a hit, and the requirement for fusing to occur relatively close to these small and relatively agile systems, demonstrates the futility of

using ballistic propagators (bullets) or blast generated fragments as a method of damaging a small UAS. And this assessment portrays a best case scenario where there is no overlap between components or shielding and where the fragment is provided a planform view normal to the path of travel. This idealized case is extremely unlikely to occur in real-world engagements. As such, the employment of kinetic propagators must be ruled out. This analysis suggests the study of alternative kill mechanisms is necessary.

C. KILL MECHANISM ANALYSIS

Where high velocity grains were shown to be have a low likelihood of inflicting damage, other modes of effecting an attrition or mission kill can be considered.

1. Severing Communications Links

Severing communications links can interrupt flight control and guidance, or video feedback to the operators. If the weaponized payload is command activated, it could prevent fusing/activation of onboard explosives. However, as detailed in Chapter I, the onset of low-cost processors suited to autonomous operations may render such a kill mechanism ineffective. Drones can be designed to fly pre-programmed routes or to execute pre-programmed manoeuvres to both minimize susceptibility or in response to a loss of communications. Some commercial UAS already demonstrate this capability with a programmable "return to home" function, which instructs the platform to fly to a pre-determined geographic coordinate in the event of a loss of communication with operators [28]. As such, simply severing communications/command links would be ineffective in eliminating the UAS threat.

2. Electromagnetic Energy Exposure (EMP)

Electromagnetic pulses could be used to overwhelm unshielded electronics onboard a UAS. Recent advances in electromagnetic pulse (EMP) technology have resulted in the development of experimental weapons such as the Counter-Electronics High-Powered Advanced Missile Project (CHAMP), built under partnership between Raytheon and Boeing [29]. An EMP system, however, has numerous disadvantages. It increases the risk of collateral, since it is an indiscriminate weapon. As such, friendly

systems that maybe unshielded nearby also risk damage. Minimization remains a challenge, with the CHAMP designed as an area weapon that would target large areas including whole cities. It also remains to be proven that the costs of a high technology weapon such as EMP devices can be achieved with cost parity approaching that of a conventional commercial UAS swarm.

3. Heat and Blast Exposure (Thermobaric)

Thermobaric weapons use intense heat and blast pressure to destroy targets. Their sizes can range from air-dropped munitions (such as the AGM-114N Hellfire II) to shoulder fired man-portable weapons (Mk. 153 SMAW) used to target bunkers and hardened structures by infantry [30] [31]. Thermobaric weapons face similar issues to EMPs. As indiscriminate weapons, the risk of damage to close operating friendly forces is substantial. The handling of explosives will also drive cost requirements substantially, resulting in a cost overmatch that is the core of the counter-UAS problem presented in Chapter I.

4. Directed Energy Weapons

Various forces are fielding kilowatt class lasers to counter threats from UAS. Aside from the cost of fielding such systems, lasers face various challenges in their employment [32]. Lasers can usually only engage a single target at a time. The lasers must maintain a specific spot on the target to allow for the rapid increase in spot temperature that thermally destroys the spot area. This results in a relatively high duration of engagement (measured in seconds) and the possibility that the spot targeted will not result in destruction of the aircraft (in a similar manner to holes punched into the foam wings or non-critical elements of UAS by fragmentation warheads) [33]. Relatively lower power lasers can also be countered through the use of materials such as reflective coatings [34].

5. Fouling and Entanglement Obstacles

Fouling and entanglement devices are already being fielded by various forces to counter low-cost and low-performance UAS [35]. Devices can range from pre-

constructed netting acting as barriers to man-portable netguns which can fire deployable nets that will foul the propulsion system of the UAS. Large nets negate the requirement for a strike on a vulnerable area. If the net can foul the propeller or be wrapped around the UAS, it is highly likely to result in sufficient loss of thrust or destabilization (in the case of multi-rotor systems) to result in an attrition kill. With sufficient development, fouling mechanisms could be combined with other mechanism ranging from heavy weights to energized wires passing high voltage through the UAS.

There are numerous advantages to deploying a fouling or entanglement device. Such devices are scalable, reusable in some circumstances, can be tailored to a delivery system and involve little to no handling of explosives. These inherent advantages ensure cost-parity that should reduce the severe cost-overmatch faced by today's systems. Employing a non-destructive kill mechanism also affords the opportunity for recovery of threat UAS systems for the purposes of intelligence collection.

6. PK|H Determination for a Fouling Mechanism

Since a fouling mechanism is usually targeting the propeller, the vulnerable area changes substantially. Consider the representative threat system. With a 305 mm diameter, the propeller of the system has a disk area of 0.2922 m^2. The frontal area presented by the flying wing body was constructed based on some assumptions and given data:

- 1500 mm wingspan
- 20 cm chord length (based on similar airfoils operated by the NPS CRUSER group)
- 2.4 cm uniform airfoil thickness based on 12% thickness to chord ratio [36].
- A slung RPG-7 that is presenting a disk of 40 mm diameter.
- A propeller that completely covers the fuselage body (negating its area), due to co-axial placement of the propulsion system.

Based on these assumptions, the frontal area excluding the propeller disk was found to be 0.33 m^2. Considering the propeller as the sole vulnerable area in the frontal plane, suggests a very high vulnerability to damage to the propeller:

$$P_{K|H} = \frac{A_V}{A_P} = \frac{0.2922}{0.3300} \approx 0.8854 \quad (12)$$

Similarly, approaching a multi-rotor (such as a quadcopter) from above the rotor disks' plane would present a substantial vulnerable area with the sum of the rotor disk areas dominating the total presented area.

V. SUBMUNITIONS AND KILL MECHANISM DEVELOPMENT

A. CONCEPT OF OPERATIONS (CONOPS)

In order to develop and deliver kill mechanisms effectively, the framework under which such a weapon system is employed must be defined. This framework is referred to as the concept of operations. The CONOPS covers all the events in the kill chain which can be broadly grouped into four phases of the engagement:

1. Detection

In the detection phase, early warning sensors provide an indication of the presence of threat systems (individual or swarm) inbound. For the case of this development, the presumed sensor was the CM202U Gimbal electro-optical turret integrated with the X-MADIS (Mobile Air Defense Integrated System), developed by Ascent Vision. The system asserts a detection range for UAS based on size and motion of 2–3 km [24].

2. Acquisition and Targeting

This is the phase during which a threat is identified, its track is passed to a weapons system and a solution is computed. The X-MADIS system asserts an identification range of 382m. Depending on rules of engagement, this may be lowest range at which a delivery vehicle may be launched.

3. Launch and Delivery

A delivery vehicle is launched and flies to an appropriate separation point. For a swarming threat, this would be at a "perch point," a location at a relative azimuth and altitude to the swarm's centroid, which would allow submunitions to successfully intercept several incoming threat systems. While at the perch point, the delivery system releases submunitions based on a pre-determined engagement strategy which considers the speed of incoming threat systems, the possibility of re-engagement, and other factors.

4. Intercept

Submunitions take up a track that would intercept the target at a pre-determined point in space (proportional navigation) or a track that would result in overtaking the target (pursuit guidance). When the submunition is sufficiently close to the threat, fusing sensors activate the kill mechanism to deploy and effect a kill.

5. Twin Engagement Scenarios

Assuming the seeker has a 30° field of view, at an altitude where the delivery vehicle is 457m (1500 ft) over the swarm centroid, results in a sight radius of 123m (402 ft) laterally. The approximate geometry of the engagement is depicted in Figure 7.

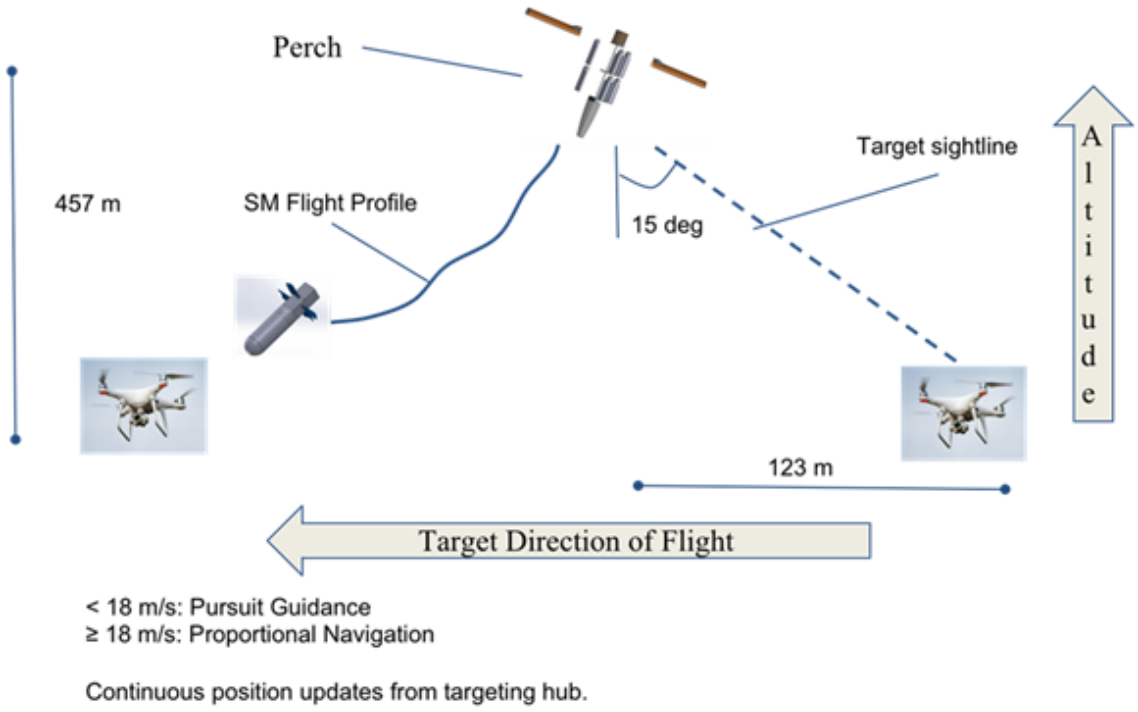

Figure 7. Engagement geometry.

As such, the intercept has to take place within a FOV of a diameter of approximately 244m (800 ft). The profiles are summarized in Figure 8.

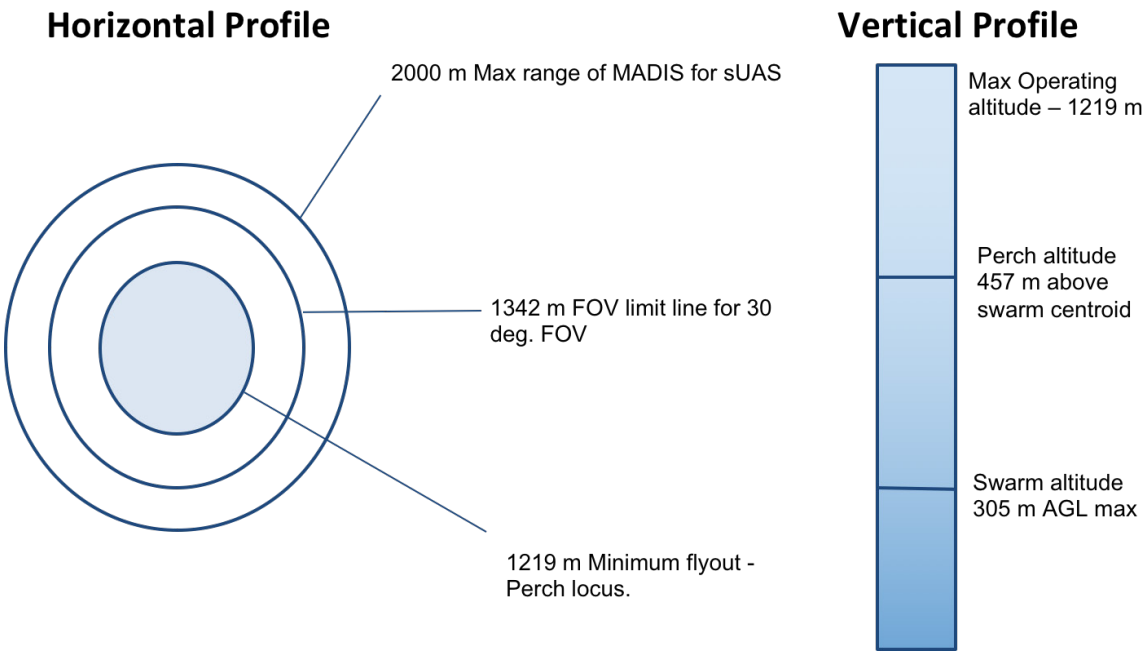

Figure 8. Vertical and horizontal profiles of minimum range intercept.

Given that terminal velocity for the submunition was estimated at approximately 55 m/s (123 mph) through numerical simulations, this would indicate a maximum velocity of approximately 198 km/h. To achieve terminal velocity, the submunition would have a distance of 154m (505 ft) and time of 5.6s, determined using kinematics:

$$v = v_0^2 + \mathrm{gt} \tag{13}$$

$$v^2 = v_0^2 + 2\mathrm{g}\Delta z \tag{14}$$

where $\mathrm{g} = 9.81\ \mathrm{m/s^2}$, $\mathrm{V_0} = 0\ \mathrm{ft/s}$, $\mathrm{V} = 55\ \mathrm{m/s}$.

The total time for the submunition to descend 457m would be a minimum of 11.12s. As such, targets or swarms traveling at speeds greater than 22 m/s, would result in the target exiting the FOV before the submunition would be able to execute a successful intercept. As such, it was decided to bifurcate the concept of operations to operate under two threat scenarios. The threshold was decided to be 18 m/s (approximately 65 km/h or 40 mph).

The velocity of the swarm determines the actions undertaken by the delivery vehicle at the perch point as shown in Table 12.

Table 12. Engagement scenarios and tactics.

Low Speed (< 18 m/s)	**High Speed (≥ 18 m/s)**
Delivery vehicle arrives at perch point, stabilizes and waits for acquisition of incoming targets before releasing submunitions. Submunitions employ pursuit guidance to intercept targets.	Delivery vehicles arrives at perch point, stabilizes and immediately releases submunitions. Targeting hub onboard the Delivery vehicle await target acquisition while the submunitions descend. Submunitions employ proportional navigation guidance to intercept targets.

B. SUBMUNITION DESIGN

A low-cost bomblet was designed using CAD software (SolidWorks) to package servos for control, a video camera, and transmitters and receivers for video links and flight control. These components were mounted in a custom designed housing, with an electronics mounting board and servo housing that were manufactured using three dimensional (3D) FDM additive manufacturing. Control was enabled using printed slatted fins, which were designed on SolidWorks and analyzed using SolidWorks Flow.

1. Submunition Aerodynamic Analysis

The bomblet was analyzed for several aerodynamic considerations, using SolidWorks Flow Simulation, a potential flow solver, to provide approximations for comparative analysis. The first consideration was to determine the terminal velocity of the bomblet. The second was to determine whether grid or slatted fins were more

appropriate for control of the submunition. And finally, to determine body forces on a submunition body modified to take a payload.

a. Terminal Velocity Determination

To determine the terminal velocity of the submunition, a basic submunition design (shown in Figure 12) was studied at various flow velocities in the direction of travel. Results are shown in Table 13. Terminal velocity was found when the drag forces were equal to the gravitational forces. For a starting mass of 0.522 kg, the approximate velocity was found to be 55 m/s (~123 mph).

Table 13. Submunition terminal velocity determination using SolidWorks Flow.

Speed (m/s)	GG(X)	GG(Y)	GG(Z)
50	-0.0638831 N	0.409218 N	4.22513 N
55	-0.0767285 N	0.507823 N	5.09617 N
56	-0.0909843 N	0.540735 N	5.28914 N
60	-0.105083 N	0.60961 N	6.06636 N
Gravitational Forces			
Mass (g)	522	Target Drag (N)	5.12082

Note: Highlighted cells are the points of comparison between calculated drag and SolidWorks Flow approximation.

b. Fin Selection

Two types of fins were considered for control of the submunition: a grid fin depicted in Figure 9 and a slatted fin. SolidWorks Flow was used to determine forces

acting on the individual fins. Angle of attack was simulated by varying the flow field from the normal direction to the surface of the fin.

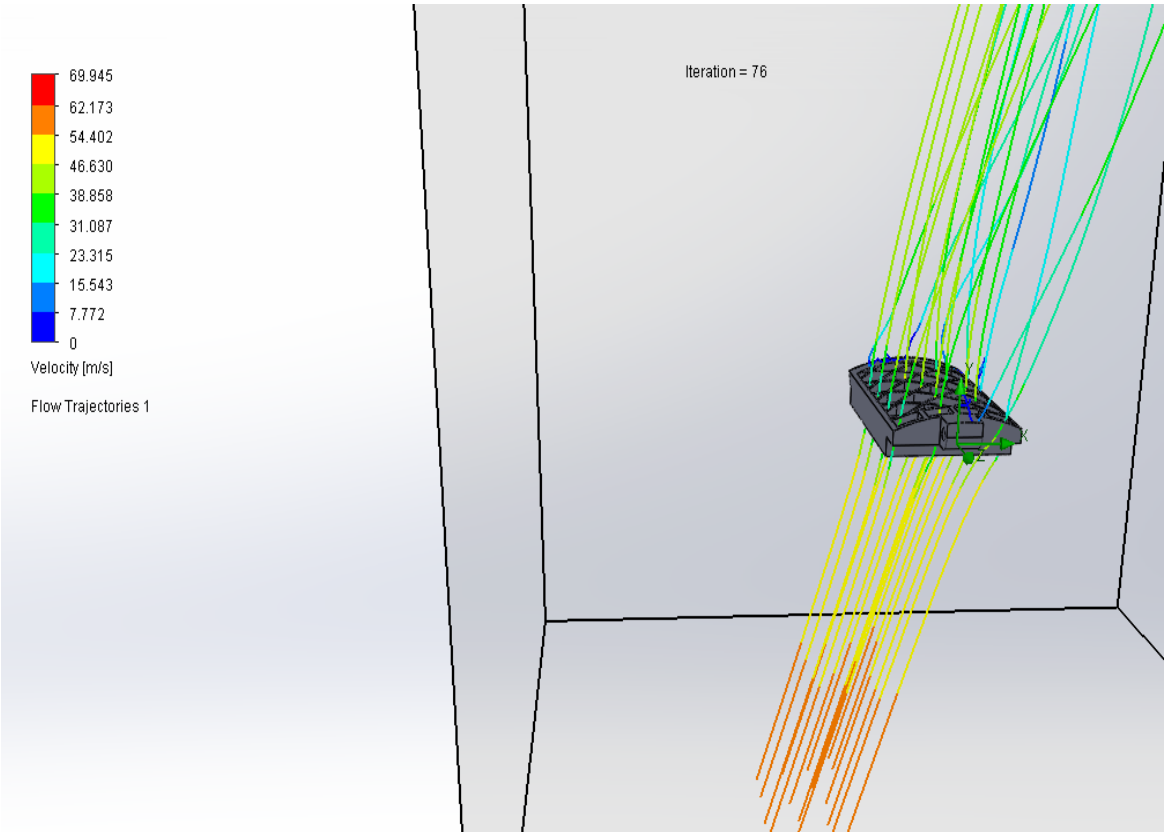

Figure 9. Grid fin modelling in SolidWorks Flow.

Lift and drag forces were analyzed for both the slatted and grid fins, and plotted in Figure 10 and Figure 11.

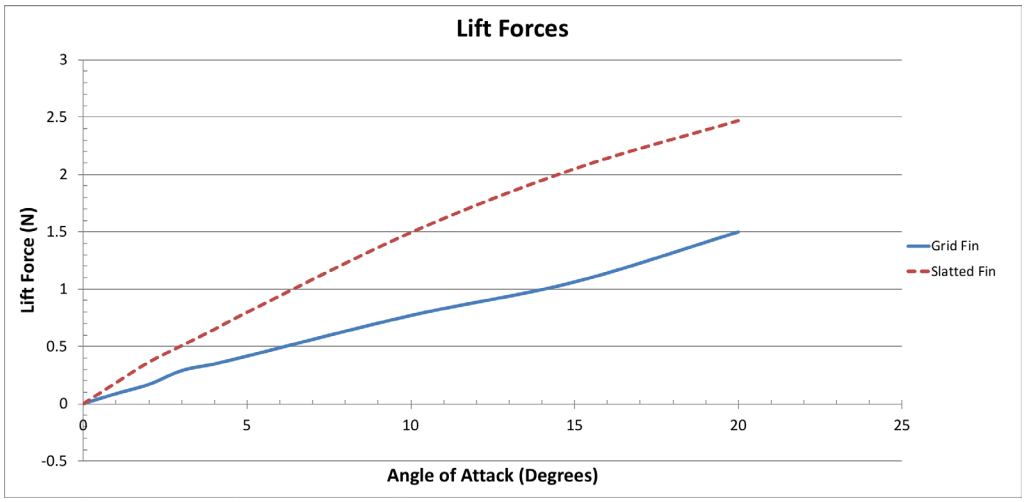

Figure 10. Lift forces on fin design

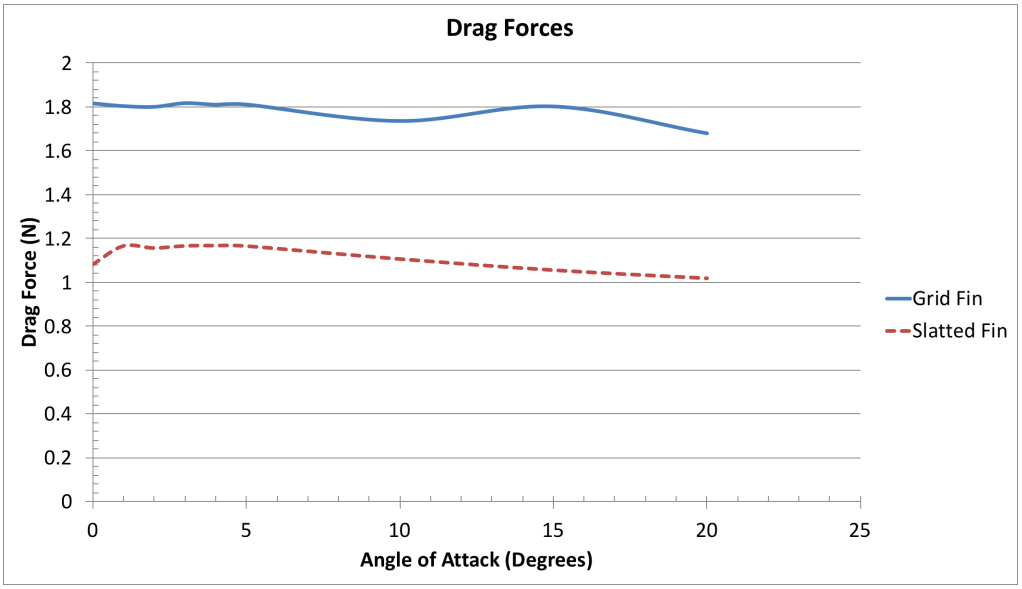

Figure 11. Drag forces on fin design.

The SolidWorks Flow analysis revealed that slatted fins were more suitable for the bomblet since they generated less drag and produced more lift compared to the grid fins. These higher lift forces could be used to generate higher turning moments on the bomblet.

c. Body Forces

To study body forces, an approximate model was constructed, shown in Figure 12 using the dimensions of the kill mechanism, to construct a payload area behind the nose cone.

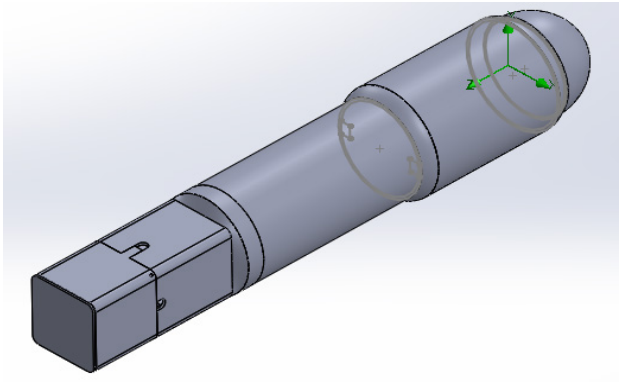

Figure 12. Initial submunition design used for SolidWorks Flow analysis.

Body lift and drag forces were analyzed at different angles of attack, as shown in Figure 13 and Figure 14.

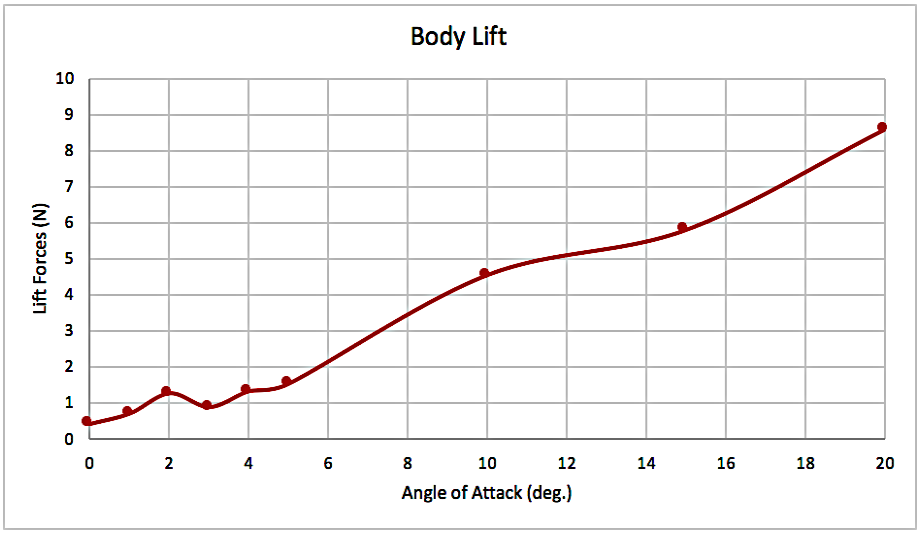

Figure 13. Lift force on submunition body.

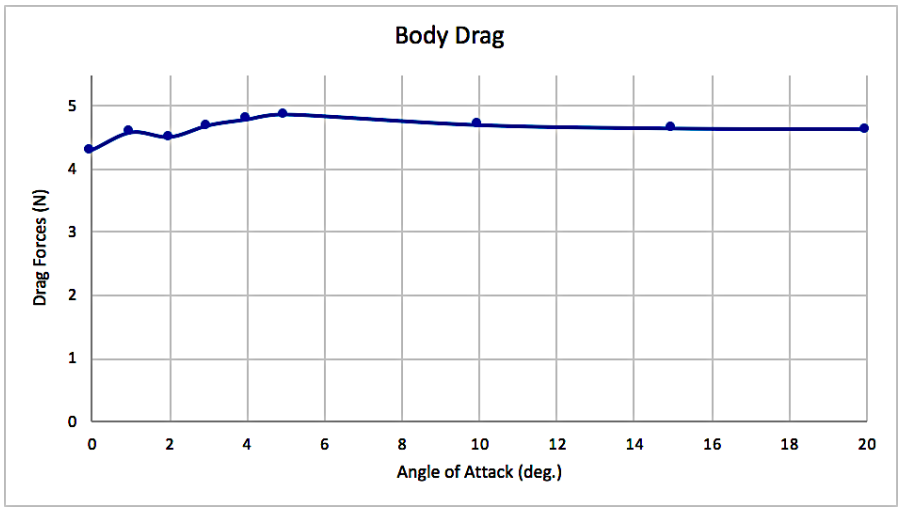

Figure 14. Drag forces on submunition body.

This analysis shows that drag tends to remain approximately constant through most angles of attack, while lift changes substantially. This analysis could be used to inform maneuvering schema such as high lift flight profiles to reduce the rate of descent.

2. Bomblet Design

The final submunition design was a "bomblet" designed and built by Robert Wright at the NPS Rocket Lab to package all the required components.

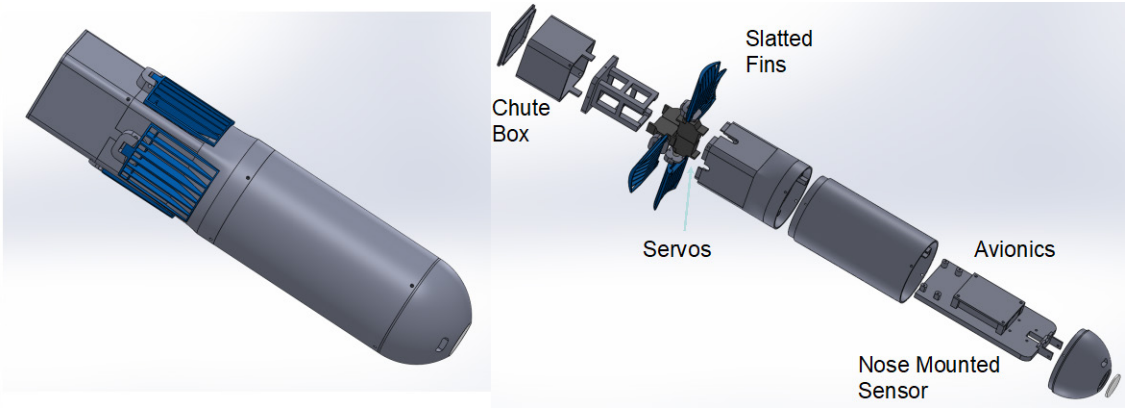

Figure 15. SolidWorks model of bomblet designed by Robert Wright at NPS Rocket Lab

The bomblet aimed to package several low-cost components listed in Table 14.

Table 14. Bill of Materials (BOM) for bomblet with approximate costs

Component	Qty.	Approx. Unit Cost ($)
Futaba S3154 High-Torque/High-Speed Servos	4	55
Luminere 600 mW transmitter	1	50
Spektrum AR400 receiver	1	30
Omnidirectional right-hand polarized antenna	2	40
PerfectFlite Stratologger CF deployment altimeter	1	50
Lithium-Polymer 500 mA 2-cell battery	1	25
MicroSD Card	1	30
RunCam Split Mini 2 FPV HD Camera	1	80
Additive printing plastics reel	1	50
Screws, pins and custom springs	As req.	0.25

As can be seen in Table 14, the approximate cost of components used in the bomblet was $625. And the form factor ensured that the four of these devices could be fit into a 191 mm (7.5 in.) diameter standard rocket tube, used by the NPS Rocket Lab as the proposed delivery vehicle. Custom parts were manufactured using additive manufacturing ("3D printing") employing an Ultimaker 3 Extended printer and its proprietary Cura software (version 3.4.1).

C. KILL MECHANISM DESIGN

A kill mechanism was designed to deploy a net as a fouling mechanism. A conical housing for a net was placed on top of a combustion chamber with passages to four chambers containing machined brass weights. An electrically activated fuse (E-Match) was used to ignite black powder in the combustion chamber. Expanding gases caused by the deflagration of the black powder displaced the brass weights at high velocity, spreading the 3.3 m^2 (36 ft^2) Dyneema net and deploying it in the direction of the

longitudinal axis of the kill mechanism. The mechanism was designed on SolidWorks and manufactured using additive manufacturing on the Ultimaker printer.

Two designs were tested. The first design (shown in Figure 16) was a proof of concept, designed to ensure that the plastic used to manufacture the kill mechanism could survive the forces of the expanding gases created by combustion of the black power.

Figure 16. Initial kill mechanism design fitted with brass weights and packaged Dyneema net

The second design (shown in Figure 17) was designed for repeatable testing and was fitted to a flight test rig, designed to be dropped from altitude, with other bomblet components (body tube, altimeter, receiver, E-match and controller, slatted fins and parachute assembly).

Figure 17. Second kill mechanism design fitted with drop test rig

D. DELIVERY VEHICLE

The delivery vehicle to be employed was a rocket previously designed by Capt. Kai Grohe (RCAF) as part of his thesis work at NPS. The main body of this rocket is a fiberglassed phenolic tube of 191 mm (7.5 in) internal diameter from Public Missiles. The BOM costs for this rocket with its motor, servos, avionics, fins and other structural elements was estimated at $4300 in 2017 [16]. This rocket was modified to enable the fitting of four bomblets internally with a payload bay which would release the bomblets during separation from the booster. Subsequently, for testing purposes, a single bomblet stowage tube was installed in the nose fairing instead of the payload bay.

VI. TESTING CAMPAIGN

Several tests were undertaken of the kill mechanism and a single flight test of a completed submunition (bomblet) was attempted.

A. KILL MECHANISM TESTING

1. Proof of Concept (First Generation)

The design depicted in Figure 16 was tested with lab pneumatic air feed on 18 October 2018. It was found that the pneumatic air lines did not deliver sufficient pressure and flow rates to deploy the net. A second test was then conducted, on 19 October 2018, with approximately 1g of black powder ignited by an E-match. The net did not unfurl and proceeded to travel over 18m as a clumped mass with the brass weights entangled.

The second test, while not adequately deploying the net, did reveal that sufficient pressure could be developed in the combustion chamber to successfully separate the net and eject the brass weights at high speed. It was subsequently decided to carry forward with the concept with additional modifications to be made:

- Build the mechanism as a single mass with voided spaces for the combustion chamber and passages to the brass weights.
- Substantially enlarge the stowage space for the net.
- Substantially shrink the combustion chamber to reduce the amount of empty volume around the black powder required while maintaining sufficient pressure to deploy.

2. Flight Test Rig (Second Generation)

The design shown in Figure 17 was tested on 01 November 2018 with 0.805g of black powder used to deploy the throw weights and net. The kill mechanism, without the flight test rig is shown in Figure 18.

Figure 18. Second kill mechanism with net packaged in stowage space and held with tape.

The test proved that the modifications made from the proof of concept were much more effective in successful separation of the net, unfurling it and spreading it to a larger effective area.

A second test was conducted on 08 November, with 0.812g of black powder, and with a cover plate added to the kill mechanism, to fully enclose the net. The goal of the test was to ensure successful separation of the cover and the net. The results were mixed. The cover successfully separated and cleared the net mechanism. However, the net did not spread completely and became partially entangled. It was decided that net packing would be modified to reorder the net's main lines attached to the throw weights, so that the lines were at the front of the net stowage volume.

A third test was intended to be conducted by attaching the kill mechanism to a flight test rig using additive printed bomblet fuselage tubes, slatted fins, parachute box and a PerfectFlite altimeter for activation. However, arranging a suitable lifting vehicle for the flight test rig and finding a suitable test area proved challenging. There were also challenges fielding qualified test personnel, as NPS staff are not permitted to operate UAS flights. As such, it was decided to conduct a nose-down static test from the roof of the NPS Rocket Lab, on 27 November 2018. The flight test rig was tied to a rod extended from a ladder, with a height of approximately 5.2m (17 ft.), as shown in Figure 19.

Figure 19. Nose-down deployment test configuration.

The kill mechanism was remotely activated using electronics similar to that which would be used during a flight test. The test was captured with a high-speed camera. Figure 20–23 show the sequence of deployment.

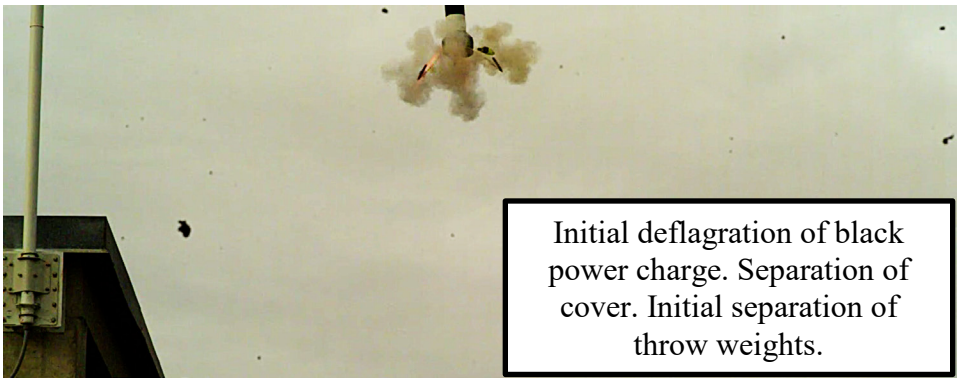

Figure 20. Flight test rig net firing 1.

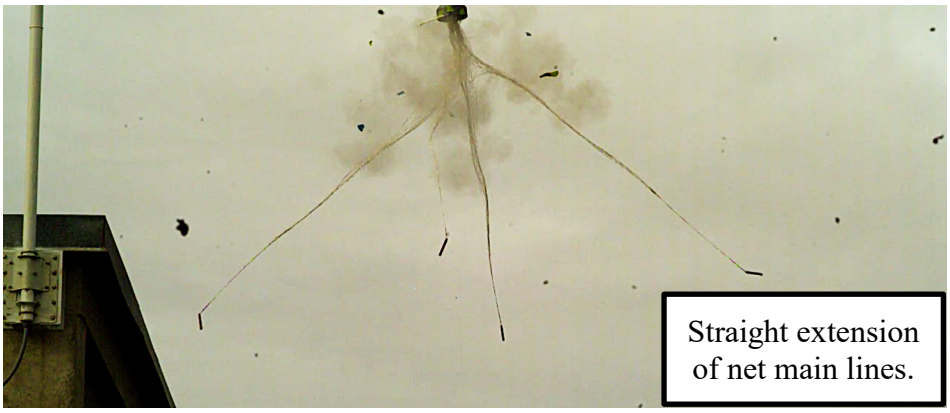

Figure 21. Flight test rig net firing 2.

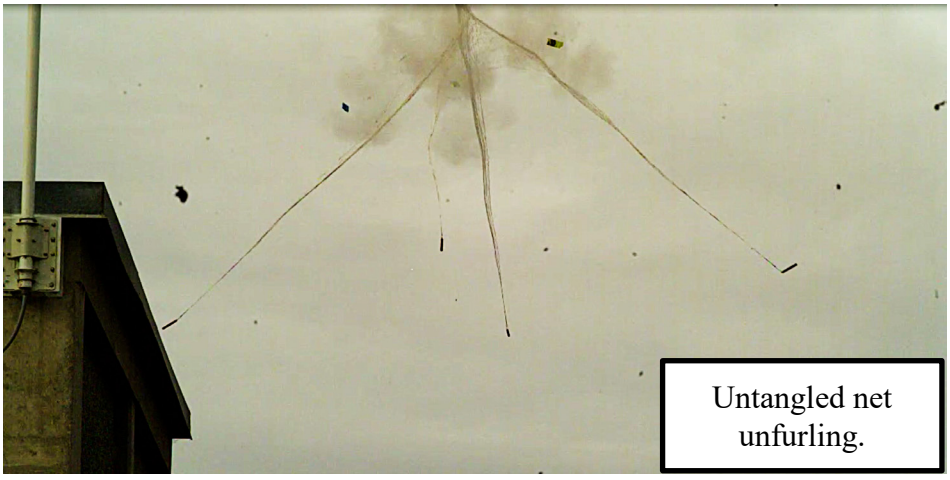

Figure 22. Flight test rig net firing 3.

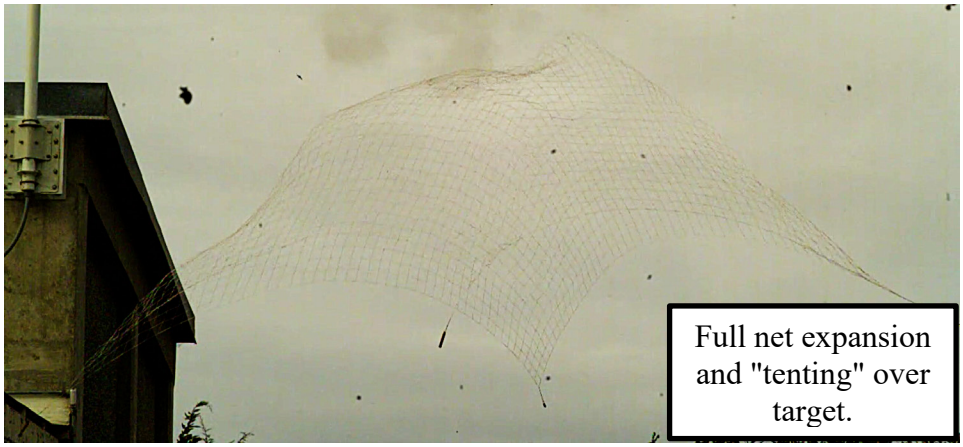

Figure 23. Flight test rig net firing 4

These images show a clean separation of the kill mechanism cover, straight lines to the throw weights and an even and untangled deployment of the net over a large area. Such a deployment, in an operational context, would have a high likelihood of success against a threat drone.

B. BOMBLET TESTING

To test the submunition, the bomblet was mounted on top of a 191mm diameter rocket and launched at the Friends of Amateur Rocketry site, in Randsburg, California. The intent was to demonstrate successful separation of the submunition from the delivery vehicle and controlled flight through visual guidance from the ground, based on imagery from the onboard camera. The mounting of the bomblet is depicted in Figure 24 and Figure 25.

Figure 24. Nose-mounted submunition

Figure 25. Nose-mounted submunition on rocket in launch configuration.

The test was unsuccessful due to the bomblet departing the rocket prior to the rocket attaining apogee. And while it provided continuous video during its descent, the bomblet was unable to demonstrate control responsiveness. Reviewing footage from the bomblet (Figure 26) and cameras on the rocket (Figure 27), damage to the rocket nose cone (Figure 28) and from analysis of the bomblet wreckage (Figure 29), it was discovered that bomblet broke into two pieces, at the join of the servo housing and the avionics bay. The front half of the bomblet departed the rocket early, while the servo section remained on the rocket till it was ejected at apogee by the separation mechanism as planned. The lack of a pressure relief port in the stowage tube for the bomblet caused the bomblet to rise in the tube which resulted in partial deployment of the fins (as seen in Figure 26). It is likely that shear forces experienced as the rocket accelerated and pitched, resulted in the structural failure which broke the bomblet.

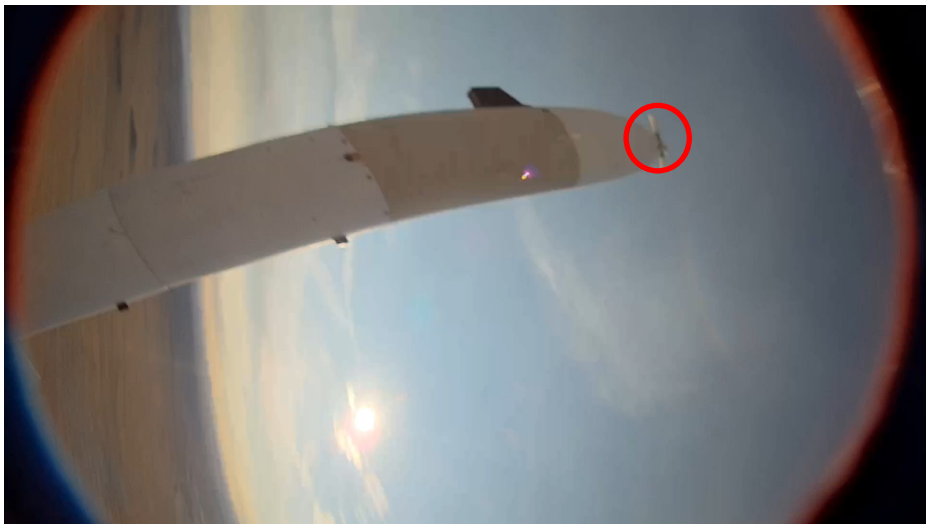

Figure 26. Servo section with partially deployed fins, remaining on the rocket, as seen from the submunition camera.

Figure 27. Front half of the bomblet falling away from rocket as seen by rear-facing camera mounted on rocket.

Figure 28. Gouging caused in the submunition stowage tube by the departing bomblet.

Figure 29. Bomblet front half debris field at impact location.

Despite the failure of the test, the survival of some structural components and operability of electronic components throughout the structural failure and crash would indicate that the design is worth further exploration. Future testing, would ideally include a graduated testing campaign starting with drop tests from a multicopter, to an eventual repeat of the separation and deployment tests attempted at this launch.

VII. CONCLUSIONS

A. SUMMARY

The evolution of low-cost avionics and higher performance UAS available to the public has inevitably led to the weaponization of commercially available UAS and will likely lead to the employment of offensive swarms of such vehicles in the future. Successfully countering such a threat will require defenses which address both the tactical consideration of potentially overwhelming numbers, and the strategic consideration of cost asymmetry.

To understand the threat, Survivability methodology was employed to study the susceptibility of small UAS and assess the vulnerability of a representative threat. This analysis was used to inform the Concept of Operations for the employment of a low-cost small UAS counter swarm system consisting of a Delivery Vehicle, Submunitions and Kill Mechanism.

Since affordability was a major consideration of this research project, the development of the system took advantage of low-cost processes (such as additive manufacturing) and publicly available hardware (COTS, hobby grade, etc.). As demonstrated, it would be possible to develop a submunition that could target a threat UAS for less than $600 (in components), to be flown on a delivery vehicle built with approximately $4300 of components, and capable of carrying multiple submunitions.

The demonstrated kill mechanism (of a large Dyneema net to be used as a fouling mechanism), was demonstrated with several deployment tests. This mechanism can be fitted to the submunitions, with some modifications, to offer a high probability of defeating sUAS threat systems. Such designs represent major advances in the reduction of cost asymmetry and feasibility of low-cost small UAS counter-swarm weapons.

B. FUTURE WORK

Several areas of development remain to be addressed. Priority should be given to further development, testing and validation of the Wright bomblet design. Integration remains a major area of consideration with efforts required to repackage and redesign the

kill mechanism to integrate with the bomblet, along with additional study and design required to integrate a submunition carrying the kill mechanism into the delivery vehicle.

The delivery vehicle itself presents several opportunities for further study and design. The delivery vehicle may need to be redesigned based on the number of submunitions required, the tactical need for delayed deployment of the submunitions (based on changes to the CONOPS), and evolution of the sensor concept. Additionally, the separation dynamics of the submunitions from the delivery vehicles requires independent aerodynamic analysis.

Beyond further validation and testing of the Wright bomblet design, there is a requirement to improve and implement the guidance, navigation and control (GNC) systems and logic. While ground control is acceptable for testing, operational deployment would require the development of specific GNC concepts.

Finally, there is the opportunity for the exploration of lethality enhancements to the kill mechanism. These could range from material selection or construction to dramatically increase aerodynamic drag once attached to the target drone, to the incorporation of a charge device to pass high voltage charges onto the drone, disrupting onboard electrical components.

APPENDIX

Table 15. Parts list for representative threat system designed by Capt. Kai Grohe

Component	Name	Weight (kg)	Cost (USD)
Motor	Turnigy L5055A-400 Brushless Outrunner 400kv	0.293	39.13
Propeller	Master Airscrew Propeller 12x8	0.041	4.44
Battery	Turnigy Graphene 6000mAh 4S 65C Lipo Pack w/XT90	0.742	96.72
ESC	TURNIGY Basic 25amp Speed Controller w/BEC	0.045	16.45
Avionics	3dr Pixhawk Mini	0.0382	229.99
Servos	AeroStar™ AS-463HB Standard Servo 3.95kg / 0.12sec / 45.5g	0.1362	15.48
Airframe	Skywalker X-6 FPV Wing EPO 1500mm (Kit)	0.77	126.11
Total		**2.0654**	**$528.32**

THIS PAGE INTENTIONALLY LEFT BLANK

LIST OF REFERENCES

[1] Long, David E. "Countering Asymmetrical Warfare in the 21st Century," *Strategic* Insights Vol. 7 No. 3 (2008). https://www.hsdl.org/?view&did=487275.

[2] Liptak, Andrew "A U.S. ally shot down a $200 drone with a $3 million Patriot missile," The Verge, 16 March 2017, https://www.theverge.com/2017/3/16/14944256/patriot-missile-shot-down-consumer-drone-us-military.

[3] "Unmanned Aircraft System Airspace Integration Plan," UAS Task Force Airspace Integration Integrated Product Team, Washington, DC. 2011.

[4] DJI Inc., "Agras MG-1," accessed August 5, 2018, https://www.dji.com/mg-1/info#specs

[5] Nixon, Andrew "Best Drones For Agriculture 2018: The Ultimate Buyer's Guide," July 11, 2018, https://bestdroneforthejob.com/drone-buying-guides/agriculture-drone-buyers-guide/.

[6] Chen, Frank "China shows off drone brigade at Guangzhou Fortune Forum gala," Asia Times, December 08, 2017, http://www.atimes.com/article/china-shows-off-drone-brigade-guangzhou-fortune-forum-gala/.

[7] Saucedo, Carlos "500 Intel drones light up skies above Travis Air Force Base," ABC Channel 7 News, July 5 2018, https://abc7news.com/society/500-intel-drones-light-up-skies-above-travis-air-force-base/3714035/.

[8] "Department of Defense Announces Successful Micro-Drone Demonstration," U.S. Department of Defense, January 9, 2017, https://dod.defense.gov/News/News-Releases/News-Release-View/Article/1044811/department-of-defense-announces-successful-micro-drone-demonstration/.

[9] "Perdix Fact Sheet," Strategic Capabilities Office - Office of the Secretary of Defense, accessed October 1, 2018, https://dod.defense.gov/Portals/1/Documents/pubs/Perdix%20Fact%20Sheet.pdf?ver=2017-01-09-101520-643.

[10] "Video reportedly shows ISIS drone dropping bomb on Iraqi tank," Herald Sun, March 24, 2017, https://www.heraldsun.com.au/news/world/video-reportedly-shows-isis-drone-dropping-bomb-on-iraqi-tank/video/807ba3094fc14299b94636ce0a440fcd.

[11] "Drone Parts and Components," Medium Inc., June 16, 2016, https://medium.com/@UAVLance/drone-parts-and-components-15582f68e920.

[12] Kobielus, James "Low-Cost AI Chipsets Will Take the Mobility Market by Storm in 2018," January 16, 2018, http://www.dataversity.net/low-cost-ai-chipsets-will-take-mobility-market-storm-2018/.

[13] Ordoukhanian, Edwin and Madni, Azad M. "Resilient Multi-UAV Operations: Key Concepts and Challenges." *54th AIAA Aerospace Sciences Meeting*, AIAA SciTech Forum. AIAA 2016–0475. San Diego, CA, 2016. https://arc.aiaa.org/doi/10.2514/6.2016-0475.

[14] Ball, Robert E. *The Fundamentals of Aircraft Combat Survivability Analysis and Design, Second Edition*. American Institute of Aeronautics and Astronautics, Reston (2003).

[15] "Design and Build Your Own Electric RC Airplane," Autodesk Inc., accessed October 05, 2018, https://www.instructables.com/id/Design-Build-Your-Own-Electric-RC-Airplane/.

[16] Grohe, Kai. "Design and development of a counter-swarm prototype air vehicle." Master's Thesis. Naval Postgraduate School, Monterey, California, 2017. https://calhoun.nps.edu/handle/10945/56932.

[17] C. J. Li and H. Ling, "An Investigation on the Radar Signatures of Small Consumer Drones," *IEEE Antennas and Wireless Propagation Letters,* vol. 16, pp. 649–652, 2017.

[18] White, Jack R. "Aircraft Infrared Principles, Signatures, Threats, and Countermeasures," Naval Air Warfare Center Weapons Division, Point Mugu, 2012. http://www.dtic.mil/dtic/tr/fulltext/u2/a566304.pdf.

[19] Zheng, Haijing and Bai, Tingzhu and Wang, Quanxi and Cao, Fengmei & Shao, Long & Sun, Zhaotian. "Experimental Study of Multispectral Characteristics of an Unmanned Aerial Vehicle at Different Observation Angles." *Sensors* Vol. 18 Issue 2 (2018). DOI 10.3390/s18020428. https://www.mdpi.com/1424-8220/18/2/428.

[20] "Zafiro HD-MW," accessed August 20, 2018. https://www.leonardodrs.com/media/4275/zafiro_hd-mw_datasheet.pdf.

[21] Love, John. "How to assess thermal camera range capability for site design purposes," accessed August 20, 2018. http://www.drsinfrared.com/Portals/0/docs/201409_TruthAboutRangeData_MR-2014-10-683A.pdf.

[22] DeFlumere, Michael E., March 08, 2005, "Dual-mode focal plane array for missile seekers." United States, US6864965B2.

[23] "OPAL," Neptec Technologies Corp., accessed August 20, 2018, http://www.neptectechnologies.com/products/opal/.

[24] Harvey, Brendan and O'Young, Siu. "Acoustic Detection of a Fixed-Wing UAV," *Drones* Vol. 2 No. 1 (2018): 4. https://www.mdpi.com/2504-446X/2/1/4

[25] Benyamin, Minas and Goldman, Geoffrey H. "Acoustic Detection and Tracking of a Class I UAS with a Small Tetrahedral Microphone Array," Army Research Laboratory, 2014. http://www.arl.army.mil/arlreports/2014/ARL-TR-7086.pdf.

[26] "CM202U Gimbal," Ascent Vision, accessed November 2, 2018, http://www.ascentvision.com/cm202u-gimbal.html.

[27] "Skywalker X-6 FPV Wing EPO 1500mm (Kit)," accessed November 01, 2018, https://hobbyking.com/en_us/skywalker-x-6-fpv-wing-epo-1500mm-kit.html.

[28] "How to use DJI's Return to Home (RTH) Safely," DJI Support, August 30, 2017, https://store.dji.com/guides/how-to-use-the-djis-return-to-home/.

[29] Lewis, Brandon "Raytheon EMP weapon tested by Boeing, USAF Research Lab," OpenSystems Media, October 10, 2018, http://mil-embedded.com/news/raytheon-emp-missile-tested-by-boeing-usaf-research-lab/.

[30] "Introduction to Crew Served Weapons B3M4078 Student Handout," United States Marine Corps, accessed October 20, 2018, https://www.trngcmd.marines.mil/Portals/207/Docs/TBS/B3M4078%20Introduction%20to%20Crew%20Served%20Weapons.pdf?ver=2015-05-07-103621-683.

[31] "AGM-114N Metal Augmented Charge (MAC) Thermobaric Hellfire," Global Security, accessed October 19, 2018, https://www.globalsecurity.org/military/systems/munitions/agm-114n.htm.

[32] Hecht, Jeff "Laser Weapons Not Yet Ready for Missile Defense," Institute of Electrical and Electronics Engineers, September 17, 2017, https://spectrum.ieee.org/tech-talk/aerospace/military/no-quick-laser-missile-defense.

[33] Peck, Michael "High-energy laser weapons target UAVs," Sightline Media Group, February 19, 2016, https://www.c4isrnet.com/unmanned/uas/2016/02/19/high-energy-laser-weapons-target-uavs/.

[34] Hambling, David "Drones Fight Back Against Laser Weapons," Popular Science, November 4, 2016, https://www.popsci.com/laser-guns-are-targeting-uavs-but-drones-are-fighting-back#page-3.

[35] Trevithick, Joseph "U.S. Air Force Buying Special Drone-Snagging Shotgun Shells," Time Inc., The Drive, March 17, 2017, http://www.thedrive.com/the-war-zone/8291/u-s-air-force-buying-special-drone-snagging-shotgun-shells.

[36] Prasetyo, Edi and Nukman, Yusoff and Aznijar, Ahmad Y. “Airfoil Design for Flying Wing UAV (Unmanned Aerial Vehicle),” *Proceedings of the 4th WSEAS International Conference on Applied and Theoretical Mechanics* , Cairo, 2008. http://www.wseas.us/e-library/conferences/2008/cairo/CD-MECHANICS/MECHANICS17.pdf.

[37] Wetzstein, Gordon “The Human Visual System, Lecture 5, EE267 Virtual Reality, Stanford University,” accessed October 23, 2018, https://stanford.edu/class/ee267/lectures/lecture5.pdf.

[38] Lappin, Joseph S. and Tadin, Duje and Nyquist, Jeffrey B. and Corn, Anne L. “Spatial and Temporal Limits of Motion Perception Across Variations in Speed, Eccentricity, and Low Vision,” *Journal of Vision* Vol. 9 No.1 (2009). DOI 10.1167/9.1.30. https://jov.arvojournals.org/article.aspx?articleid=2122525.

INITIAL DISTRIBUTION LIST

1. Defense Technical Information Center
   Ft. Belvoir, Virginia

2. Dudley Knox Library
   Naval Postgraduate School
   Monterey, California